ANL-HEP-TR-89-39

ARGONNE NATIONAL LABORATORY
HIGH ENERGY PHYSICS DIVISION

SEMIANNUAL REPORT OF RESEARCH ACTIVITIES

July 1, 1988 – December 31, 1988

ARGONNE NATIONAL LABORATORY
Argonne, Illinois
Operated for
U.S. DEPARTMENT OF ENERGY
under Contract W-31-109-Eng-38

Argonne National Laboratory, with facilities in the states of Illinois and Idaho, is owned by the United States government, and operated by The University of Chicago under the provisions of a contract with the Department of Energy.

The High Energy Physics Division Report of Research Activities is prepared from information gathered and edited by the Committee for Publications and Information.

Members: E. Berger, Chairman
J. Day
E. May
R. Blair

This report has been reproduced from the best available copy.

Available from the
National Technical Information Service
NTIS Energy Distribution Center
P.O. Box 1300
Oak Ridge, TN 37831

Price: Printed Copy A05
Microfiche A01

ANL-HEP-TR-89-39

ARGONNE NATIONAL LABORATORY

HIGH ENERGY PHYSICS DIVISION

SEMIANNUAL REPORT OF RESEARCH ACTIVITIES

July 1, 1988 - December 31, 1988

Page

Table of Contents

I.	Experimental Program	1
	A. Experimental Program: Physics Results	1
	B. Experimental Program: Experiments Taking Data	17
	C. Experimental Program: Experiments in Preparation Phase	22
II.	Theory Program	41
III.	Experimental Facilities Research	49
IV.	Accelerator Research and Development	56
V.	SSC Detector Research and Development	60
VI.	Publications	69
VII.	High Energy Physics Research Personnel	84
	Appendix A Colloquia and Conference Talks	85
	Appendix B HEP Community Activities	89

High Energy Physics Division Semiannual Report of Research Activities
July 1, 1988 - December 31, 1988

I. EXPERIMENTAL PROGRAM

A. Physics Results

1. Collider Detector at Fermilab

Several Physical Review Letters have been written on the 1987 CDF data. These include the inclusive single particle momentum spectrum in minimum bias events, the inclusive jet cross section, the $W \to e\nu$ cross section, SUSY limits, and dijet angular distributions. A letter on single direct photon production is in preparation.

As of this writing, the 1988 data sample already exceeds 3 pb^{-1}, and analyses are underway on inclusive production of jets and leptons, and on the potentially interesting final states that include jets + leptons and dileptons. As examples, Fig. 1 shows the inclusive jet P_t spectrum from the 1988 sample, compared with the 1987 results and theoretical predictions. The spectrum extends to 300 GeV with good statistics, and will allow us to extend the compositeness scale limit to ~ 1 TeV. Figure 2 shows the inclusive central electron cross section for P_t values above 7 GeV (the lowest trigger threshold). This spectrum shows a steeply falling low P_t component, and a flatter component above 25 GeV/c. The low P_t component is consistent in rate with predictions from b-$\bar{b}$ production Monte Carlos, while the high P_t events appear to come mainly from W/Z production with 0,1,2.. associated jets. A top quark below the W mass would populate the region between the "bottom" and the "W/Z" components.

Figure 3 illustrates the electron tagging, using clean $W \to e\,\nu$ events (selected on the basis of missing P_t, high electron P_t and absence of jet activity). The E/p resolution is around 6% for these (typically 35 GeV) electrons ("E" is the calorimeter energy, p the track momentum). These results imply better than the design goal of 0.2 p^2 % for the resolution on the track momentum. Figure 4 shows the invariant mass spectrum for dimuon events in the J/Psi region; the fitted mass is consistent with precision

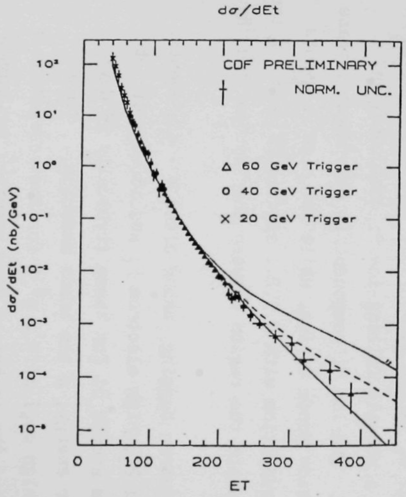

Fig. 1. Inclusive central jet spectrum from the 1988 run. The curves show QCD predictions (solid), and QCD with composite quarks (dashed, dotted curves.)

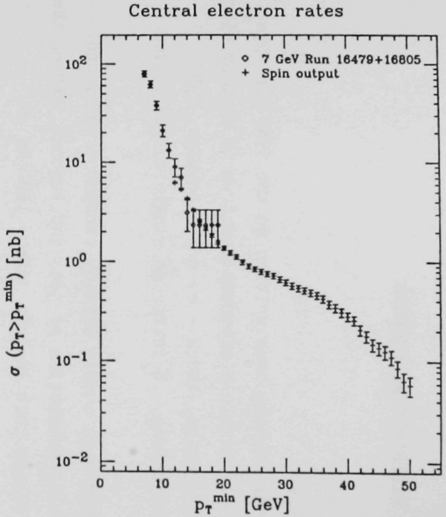

Fig. 2. Inclusive central electron integral cross section. No acceptance corrections have been applied.

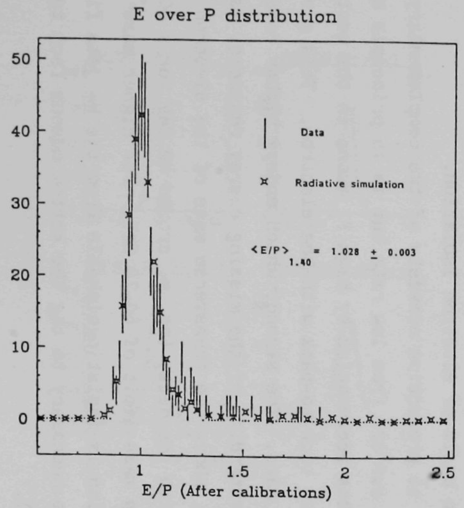

Fig. 3. E/p distribution for electrons from W decay, compared with a radiative monte carlo simulation.

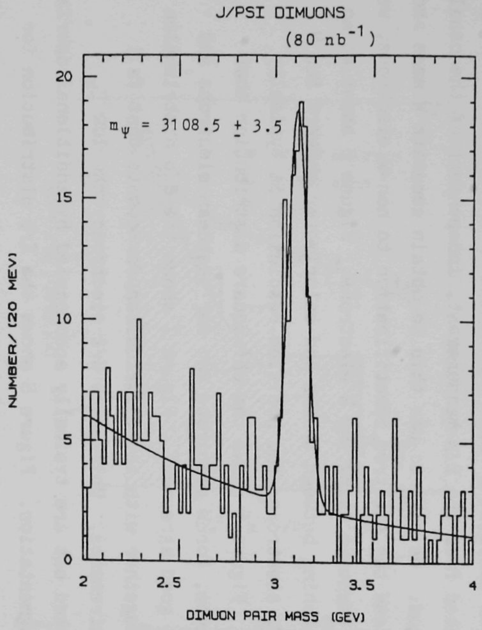

Fig. 4. Dimuon invariant mass spectrum used to calibrate the momentum scale.

measurements and serves to calibrate the momentum scale. Thus, the calorimeter energy, which includes a small contribution from brehmsstrahlung photons, can be calibrated from the E/p measurement, independent of the usual radioactive source method. We plan to use this to obtain accurate W mass and W/Z mass ratios. To extend the electron identification to non-W electrons, we calibrate the detector response using the W electrons. Figure 5 shows as an example the position-matching between tracks and calorimeter showers for W electrons and for low P_t electrons; the position resolution is typically 3-6 mm depending on P_t. Figure 6 shows the chi square distribution that describes the shower shape, for W electrons and for testbeam electrons and pions, again indicating good agreement. Figure 7 shows the E/p distribution for low P_t electrons, together with the distribution for events that fail calorimeter shower requirements. Unlike the W/Z electrons, the low P_t electrons are not isolated but are typically accompanied by additional debris from the bottom jet fragmentation. Figure 8 shows the E/p distribution for low P_t electrons, cut on the ratio of total jet energy to electron energy; the electron peak is quite clean in all samples, regardless of the degree of isolation. This indicates that bottom production can be studied via electron tagging in CDF, and bottom backgrounds to top or W/Z production can be separated statistically on the basis of electron isolation.

The strategy for finding $t\bar{t}$ production consists of two complementary selections. The first, which suffers from low rate but is in principle quite clean, is a search for electrons accompanied by high P_t muons in the central detector, where the muon is not back-to-back with the electron. This gives a limit of ~ 60 GeV for the top mass. The second, which enjoys higher rate but requires rather detailed understanding of the missing energy response, is a search for electron plus jets, where the transverse mass of the electron and its neutrino are consistent with top decay (eg, m_T around 40 GeV for a 60-GeV top). This method gives a top mass limit of 60-70 GeV. For higher mass top, the transverse mass distribution is indistinguishable from the W+ jets final state, and it will probably be necessary to tag the bottom mesons from top decay, eg. $t \to b + W$ $(W \to e\ \nu)$.

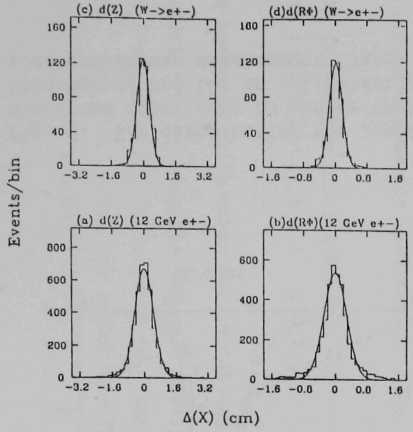

Fig. 5. Position matching distributions in z and RΦ directions for inclusive low P_t electrons (a,b) and electrons from W decay (c,d).

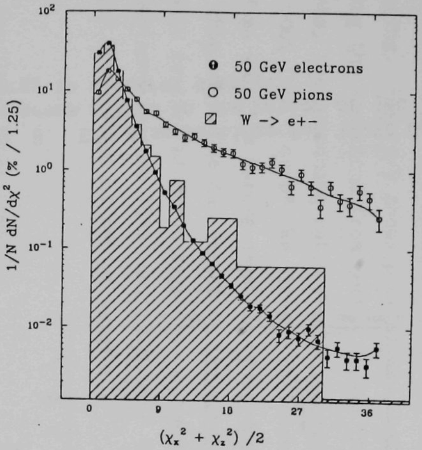

Fig. 6. Shower profile χ^2 distributions for electrons from W decay (shaded histogram), compared with testbeam electrons and pions.

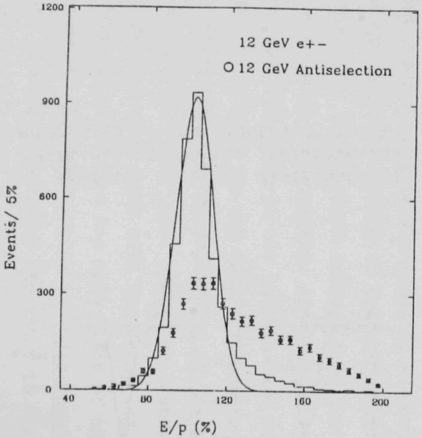

Fig. 7. E/p distribution for low P_t electrons after cuts on shower development (histogram) and for an antiselection on electron shower development (data points.)

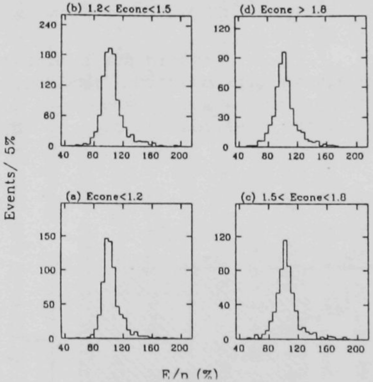

Fig. 8. E/p distributions for 12-20 GeV electrons sliced on the ration of jet energy to electron energy.

It is of considerable interest to understand in more detail the components that are visible in the electron spectrum, in order to separate cleanly the bottom and W/Z final states; this may also provide instruction in bottom tagging. Figure 9 shows preliminary results of a search for charm accompanying the electrons from bottom decays ($B \to c\ e\ \nu$); from CLEO measurements, the branching ratio for nonstrange semi-leptonic bottom meson decays is 100% into D or D*. We observe evidence for a D^o peak in the $K\pi$ channel (Fig. 9a); the "wrong sign" combinations (eg, e- with K+ π^-) show no such peak (Fig. 9b). We can expect on the order of 50000 bottom events in the 1988 run with central electron tagging. We expect that these studies will be useful experience for the 1990 run, which will feature a silicon vertex detector for more efficient bottom tagging. (A. B. Wicklund)

2. High Resolution Spectrometer

A paper "Measurement of Upper Limits for the Decay Widths of D^{*+} and D^{*o}" was published in this period. Three other papers are in press and several others exist in draft form.

A paper giving our measurements of the semielectron branching ratios for the b and c quarks as well as the forward:backward asymmetry in the reaction $e^+e^- \to b\bar{b}$ was submitted for publication. The values of:

$$Br\ (b \to ex) = (10.8 \pm 0.8 \pm 1.3)\%$$
$$Br\ (c \to ex) = (7.6 \pm 1.1 \pm 0.7)\%$$

are in good agreement with other determinations.

An analysis of the complete 300 pb^{-1} sample of data gave updated values for the one-prong (B_1) and three-prong (B_3) topological branching ratios of the τ-lepton. The data, which are summarized Table I, gave $B_1 = 0.864 \pm 0.003 \pm 0.003$ and $B_3 = 0.135 \pm 0.003 \pm 0.003$.

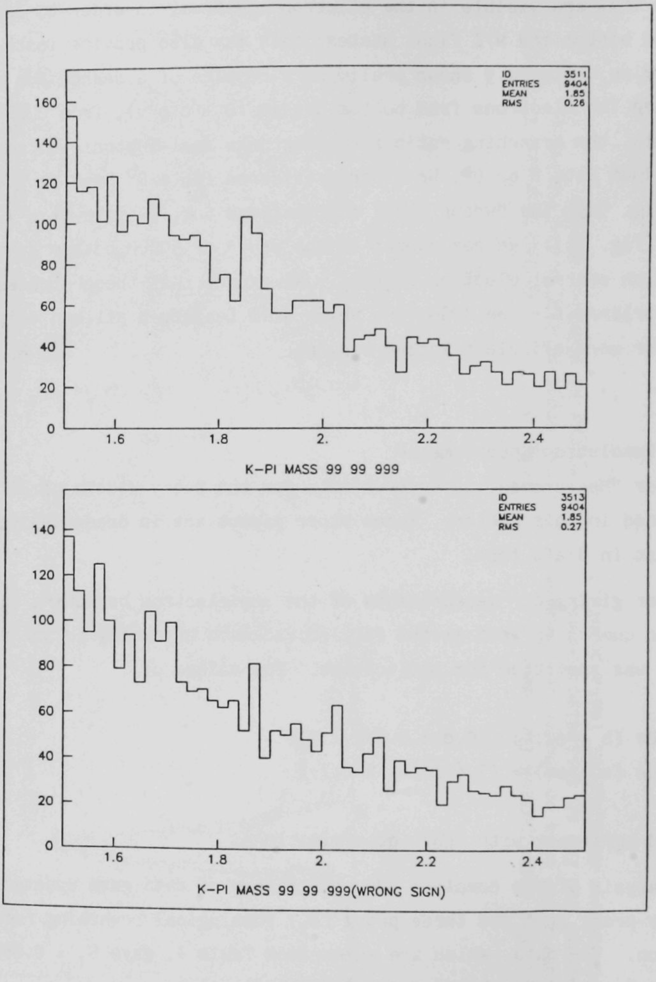

Fig. 9. K-pi mass spectra for "right sign" (top) and "wrong sign" (bottom) charged particle pairs, where the tracks are chosen from a cone surrounding the low-P_t electron.

Table I

τ-Decay Data and Background Summary

Topology	Number of Events	Background	Corrected Number of Events	Detection Efficiency
1-1	3643	(7.8 ± 0.3)%	3359	(11.07 ± 0.12)%
1-3	2693	(5.8 ± 1.1)%	2537	(26.42 ± 0.29)%
3-3	158	(7.4 ± 2.4)%	146	(21.85 ± 0.91)%
1-5	13	(1.4 ± 0.6)%	13	(15.98 ± 0.82)%

A total cross section for the reaction $e^+e^- \to \tau^+\tau^-$ at $\sqrt{s}$ = 29 GeV was also measured. When compared to the point cross section, the result was $R_{\tau\tau}$ = 1.044 ± 0.014 ± 0.030.

The complete hadronic data sample was used to study the production cross sections for the vector mesons ρ^0 and $K^{*0}(890)$. The technique consisted of fitting the neutral two particle mass distribution with contributions from the known resonances and their reflections. Each mass combination was tried as both a $\pi^+\pi^-$ combination and two $K^\pm\pi^\mp$ combinations. Figures 10 and 11 show the $\pi\pi$ and $K\pi$ distributions after subtracting the charge two combinations. The shaded areas show the contributions to the fits coming from the ρ and K^{*0} vector mesons. Figures 12 and 13 give the resulting cross sections as a function of the energy sharing variable $Z = 2E_{meson}/\sqrt{s}$. The lines are the best fits using the Lund Monte Carlo model (version 6.3). Using this model to extrapolate to threshold gives multiplicities of $n_{\rho^0} = 0.90 \pm 0.05$ and $n_{K^{*0}} = 0.63 \pm 0.10$. We have previously reported a value for the charged $K^*(890)$ of $n_{K^{*\pm}} = 0.62 \pm 0.045 \pm 0.040$. These values are in good agreement with our earlier measurements and the results reported by the PEP and PETRA collaborations as seen in Table II.

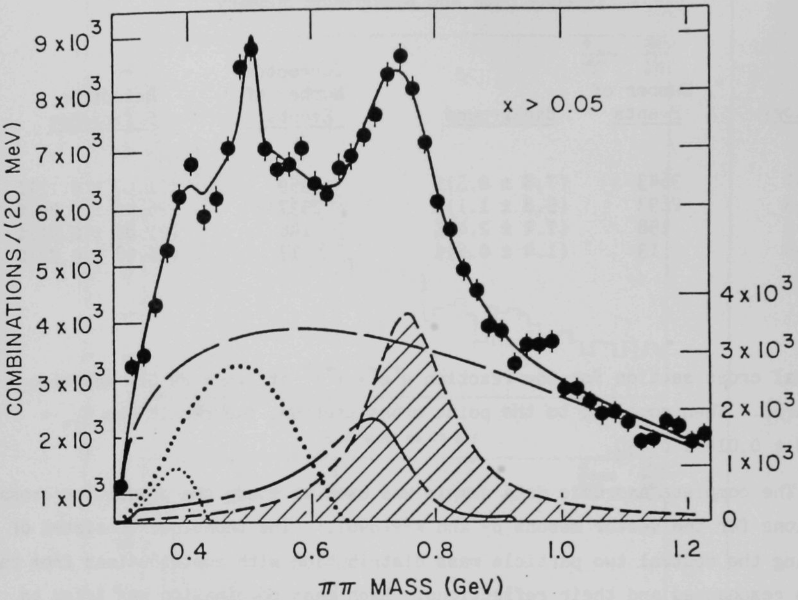

Fig. 10. Subtracted neutral $\pi^+\pi^-$ mass spectrum for $x > 0.05$. The dashed line shows the smooth background using the form given in Eq. (1) of the text. This function also well represents the doubly-charged spectra. The data, the total fit, and the above background contribution refer to the ordinate scale on the left. Four other individual contributions to the fit are shown at the bottom of the figure with ordinate scale on the right.

i) contribution from $\eta^o \to \pi^+\pi^-\pi^o(\gamma)$ decays (light dotted line);

ii) contribution from $\omega^o \to \pi^+\pi^-\pi^o$ decays (heavy dotted line);

iii) K^{*o} reflection (short-dashed-long dashed line);

iv) ρ^o contribution (hatched area). The fit also includes a contribution from $K^o \to \pi^+\pi^-$ decays where the decay occurs close to the primary vertex.

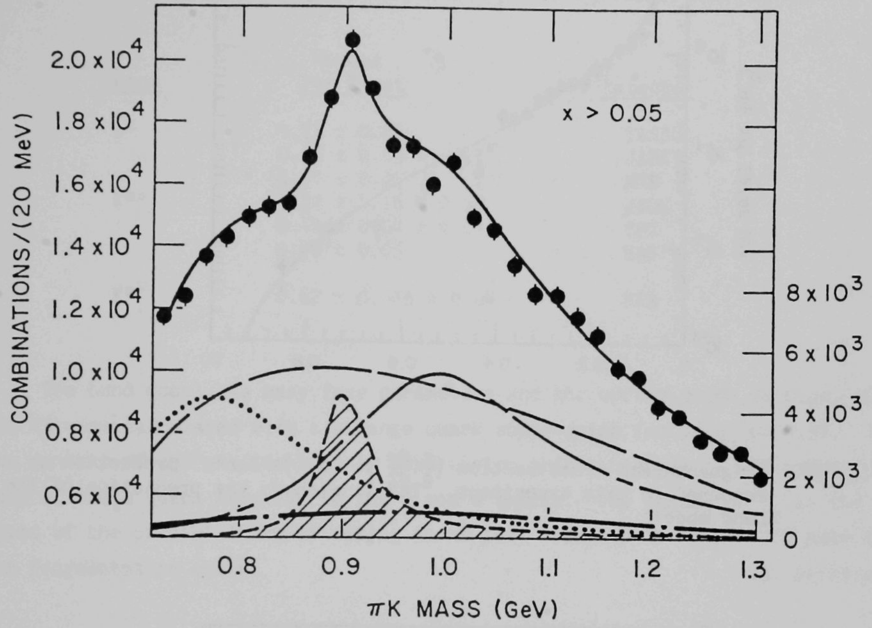

Fig. 11. Subtracted neutral $\pi^{\pm}K^{\mp}$ mass spectrum for $x > 0.05$. The dashed line shows the smooth background using the form given in Eq. (1) of the text. This function also well represents the doubly-charged spectra. The data, the total fit, and the above background contribution refer to the ordinate scale on the left. Four other individual contributions to the fit are shown at the bottom of the fig with ordinate scale on the right.

i) contribution from $\omega^{0} \to \pi^{+}\pi^{-}\pi^{0}$ with a $\pi^{\pm}$ misidentified as a $K^{\pm}$ (heavy dotted line);

ii) ρ^{0} reflection (short dashed-long dashed line);

iii) K^{*0} reflection with $K^{\pm} \leftrightarrow \pi^{\mp}$ interchanged (dashed-dotted line);

iv) K^{*0} contribution (hatched area).

The fit also includes a contribution from $K^{0} \to \pi^{+}\pi^{-}$ decays with a charged pion incorrectly assigned the kaon mass.

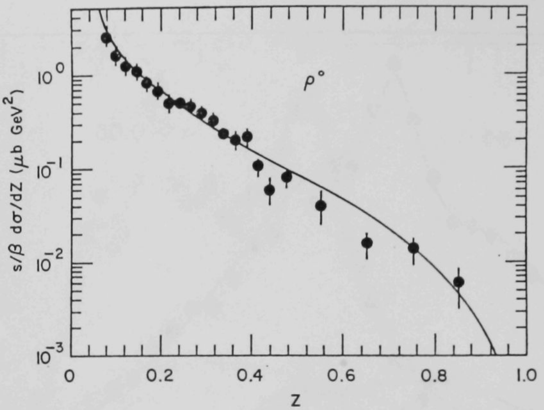

Fig. 12. Fragmentation cross section $(\frac{s}{\beta}\frac{d\sigma}{dZ}$ μb GeV$^2)$ for ρ^0 production as measured in this experiment. The line shows the prediction of the Lund model.

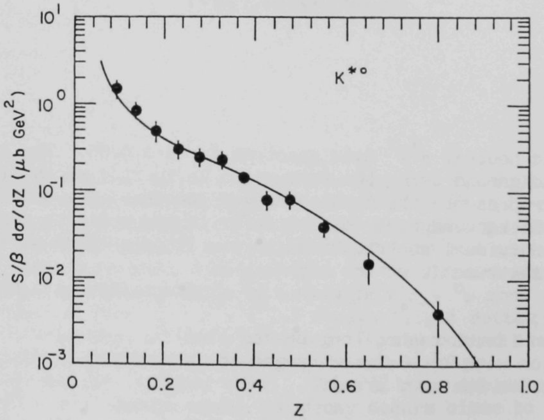

Fig. 13. Fragmentation cross section $(\frac{s}{\beta}\frac{d\sigma}{dZ}$ μb GeV$^2)$ for K^{*o} production as measured in this experiment. The line shows the prediction of the Lund model.

Table II

Multiplicities of ρ^0 and $K^{*0}(890)$ in e^+e^- Annihilation near 30 GeV.

Meson	Mesons Per Event	Detector
ρ^0	0.73 ± 0.06	TASSO
	$0.98 \pm 0.09 \pm 0.15$	JADE
	0.90 ± 0.05	HRS
K^{*0}	$0.87 \pm 0.16 \pm 0.08$	JADE
	$0.49 \pm 0.04 \pm 0.07$	TPC
	0.59 ± 0.05	HRS
$K^{*\pm}$	$0.62 \pm 0.045 \pm 0.04$	HRS

The Lund model has many free parameters and the curves shown in Figs. 12 and 13 were calculated with a strange quark suppression factor γ_s of 0.34. In the context of current ideas, this suppression arises because of the higher mass of the s quark relative to the n and d quarks. The parameter γ_s is the ratio of the probabilities of making an $s\bar{s}$ pair relative to a $u\bar{u}$ or $d\bar{d}$ pair in the fragmentation chain. (M. Derrick)

3. Computational Physics

The computational physics effort continues to be devoted to simulations of Lattice Gauge Theories with dynamical quarks. First and foremost we are continuing our simulations of lattice quantum chromodynamics (QCD) in an attempt to understand better the physics of Hadrons and Nuclear Matter. Secondly with the arrival of J. B. Kogut we have begun to study the newly found strong coupling phase of QED also using lattice simulations. In both cases we are using the hybrid (microcanonical/Langevin) algorithm for our simulations, while continuing to look for improved simulation methods. The large amounts of computer time needed are being provided by the HEP Division's ST-100 array processor, the ETA-10 at SCRI, Florida State University, CRAY X-MP's and CRAY 2S's at MFECC and NCSA, and a CRAY Y-MP at the Pittsburgh Supercomputer Center.

Our recent work on finite-temperature QCD at intermediate-large quark masses on a $12^3 \times 4$ lattice had indicated that finite-size effects on smaller lattices could obscure the true nature of the phase structure of QCD. With this in mind, we (Kogut and Sinclair) have been extending our previous studies of the small mass region to this larger lattice. A study of the phase transion for four degenerate flavors of quarks with m = 0.025 is being performed on the ST-100. A study of the phase transition with a more realistic spectrum of two light quark flavors (u and d, m = 0.0125) and one intermediate mass quark flavor (s, m = 0.25) is being done on the CRAY 2S at NCSA and the CRAY Y-MP at Pittsburgh.

We are part of a multi-institutional collaboration whose goals are to measure hadron mass spectra, including glueballs and exotics, to measure other matrix elements, such as those required to determine hadronic structure functions (in particular the spin-dependent structure functions). For these simulations we are using time on the ETA-10 at SCRI granted under the DOE's Grand Challenge initiative. With this we are able to use the large ($16^2 \times 24^2$) lattices required to perform meaningful calculations.

Recent analytic work has suggested that quenched QED posesses an ultraviolet stable fixed point. Pioneering simulations and further analytic work by Kogut with E. Dagotto and A. Kocic support these conclusions, and indicate that the fixed point survives the inclusion of dynamical fermions. This behavior of QED not only makes QED a well-defined theory in isolation, but the new strong-coupling phase defines a new theory with properties long sought after by model builders. More extensive simulations are now planned for the ST-100 by K. C. Wang, Kogut and Sinclair. The code for the ST-100 was prepared by Wang with the help of Sinclair. (D. Sinclair)

4. Spin Physics at LAMPF

In the past six months final results for the mixed spin-spin correlation parameter $C_{\sigma\sigma} \approx 0.5\ C_{SS} - 0.8\ C_{SL}$ for np elastic scattering were obtained from E-665/770 data collected in 1985. The incident neutron-beam kinetic energies were 484, 634, and 788 MeV and the center-of-mass angles ranged from about 75° to 180°. These $C_{\sigma\sigma}$ results are important for determining the I = 0 nucleon-

nucleon amplitudes and provide strong constraints on the phase shift solutions.

The measured values of $C_{\sigma\sigma}$ are shown in Fig. 14. The most recent phase-shift predictions of the VPI, Basque and Saclay-Geneva groups and the meson-exchange model predictions of T.-S.H. Lee et al. (ANL - Physics Division) and Machleidt et al. are also shown. Predictions for the pure spin-spin correlation parameters C_{SS}, C_{NN}, C_{LL}, and C_{SL} at the desired angles and energies were used, along with the spin component admixture coefficients, to calculate $C_{\sigma\sigma}$.

The reduced chi-squared (χ^2/ν) for each prediction was computed; none of the predictions included these data. At 484 MeV none of the predictions fit the data particularly well ($\chi^2/\nu > 5$), particularly for the c.m. angles larger than 150°. At both 634 and 788 MeV, the VPI and Lee et al. predictions give $\chi^2/\nu \lesssim 2.5$. In addition, the Saclay-Geneva results at 634 and the Basque results at 788 MeV satisfy this criterion. Other predictions have $\chi^2/\nu > 4$. It is anticipated that better fits to the $C_{\sigma\sigma}$ data could be obtained by modification of the present phase shifts.

A study of the I = 0 phase shifts most affected by these data was performed with the VPI program SAID. It was found that the $^1P_1$, $^3S_1$, and $^3D_1$ partial waves were most strongly affected.

Values of the pure spin-spin correlation parameter C_{SS} can be derived from the $C_{\sigma\sigma}$ data using experimental results at 484 and 634 MeV. Published data for C_{LL}, C_{SL}, and C_{NN} do not exist at 788 MeV. However, the errors on C_{SS} would be dominated by uncertainties on the other spin-spin correlation parameters, not by the $C_{\sigma\sigma}$ errors. (H. Spinka)

5. ZGS Polarized Data Analysis

A paper was submitted describing some new ZGS results on the difference between pp total cross sections for pure helicity states $\{(\Delta\sigma_L(pp) = \sigma^{Tot}(\rightleftarrows) - \sigma^{Tot}(\rightrightarrows)\}$. New data at P_{lab} = 3.75, 4.0, 5.0, and 11.75 GeV/c, together with previous ZGS and Saclay results above 2 GeV/c, reveal energy

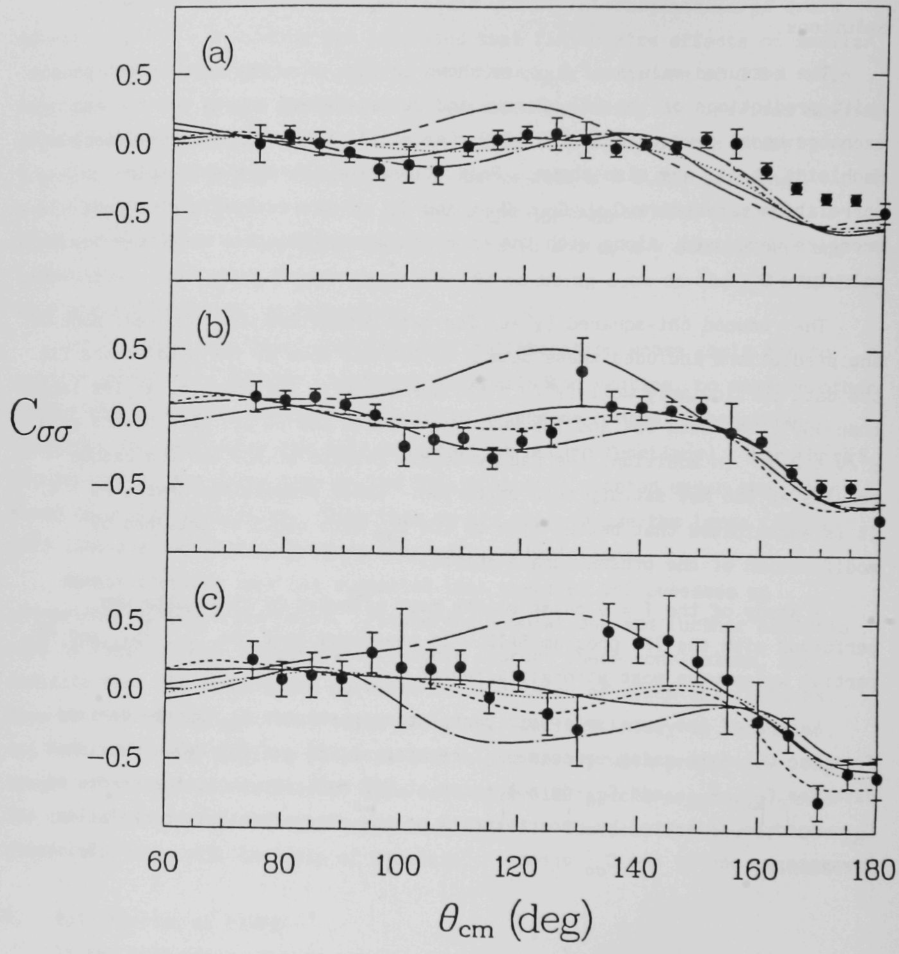

Fig. 14. Measured values of $C_{\sigma\sigma}$ for np elastic scattering at a) 484, b) 634, and c) 788 MeV. The curves are the predictions of the VPI group (Arndt et al.), solid line; the Saclay-Geneva group (Lehar et al.), dash-dot line; the Basque group (Bugg et al.), dotted line; Lee et al., dashed line; and Machleidt et al., chain-dash line.

dependent structure (see Fig. 15) in the mass range from 2700 to 2900 MeV/c^2. Although Coulomb-nuclear interference effects have been neglected, it is estimated that these would reduce the magnitude of $\Delta\sigma_L$ by less than 0.1 mb and would vary smoothly with energy.

The peak in $\Delta\sigma_L$ near 2700 MeV/c^2 may be related to the resonance-like behavior in the $^1S_0$ partial wave found in a recent phase shift analysis by N. Hoshizaki, as well as to structure in the pp elastic scattering spin-spin correlation parameters C_{LL} and C_{NN} near 90° and to a bump in the total pp cross section. Also near 2700 MeV/c^2, physicists at Saclay recently observed a peak in the pp elastic polarization and in the pp $\rightarrow$ dπ polarization. The peak in $\Delta\sigma_L$ near 2900 MeV/c^2 coincides with structure observed earlier in $k^2C_{LL}(d\sigma/d\Omega)$ at $\theta_{c.m.}$ = 90°. A Cloudy Bag model calculation of Lomon et al. and a diquark cluster model calculation of Konno et al. both predict dibaryon resonances near 2700 and 2900 MeV/c^2. (H. Spinka)

B. Experiments Taking Data

1. Collider Detector at Fermilab

The collider run at Fermilab is a spectacular success. Peak luminosity in excess of 2 x 10^{30} cm^{-2} sec^{-1} has been achieved. The level 2 (cluster hardware) trigger for CDF was brought up but the unanticipated boon in luminosity also required the level 3 (ACP farm) trigger. This was also brought on. By the end of the year the collider was producing 300-400 nb^{-1} per week and CDF was collecting about 200 nb^{-1} per week as seen in Fig. 16. By year's end 3.8 pb^{-1} had been produced of which 1.8 pb^{-1} is on tape for CDF. The detector basically performed quite well with the only disappointments being the unanticipated significant dead time of the level 0 trigger (lose one crossing after the presence of a minimum bias trigger) at about 15%, and the forward tracking chambers which were removed for inspection and perhaps repair.

The trigger now includes prescaled minimum bias, single cluster, multiple and total energy jet triggers, electron, muon and missing transverse energy triggers as well as combinations. As greater rejection is achieved, either

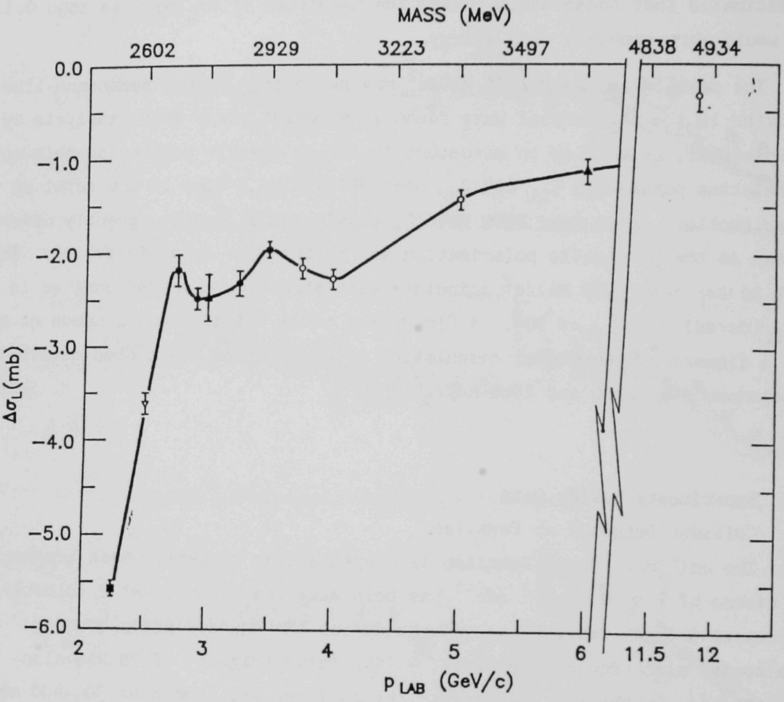

Fig. 15. The $\Delta\sigma_L$(pp) dependence on P_{lab} from 2 to 12 GeV/c. Open circles are the new results. Other data are from earlier ZGS experiments by the same experimental group. Errors shown are statistical only. The line drawn is to guide the eye.

the luminosity goes up, or additional triggers are added, or thresholds are lowered. The data rate is fairly stable at about 200 tapes per week. With considerable difficulty, the CDF reconstruction code has been brought up on ACP for regular "production." In the meantime, various real-time tight-selection passes on raw data have been consolidated into "spin" selection and production runs on VAXes on the selected samples, allowing physics analyses to get going. This status is shown in Fig. 17.

The current run is likely to continue until summer. About fifteen months from then another run with six bunches, some fraction of D^o, and perhaps a factor of five more luminosity is planned. For that run, CDF is planning to add a silicon vertex detector, upgraded central muon detection, and preradiator chambers in central calorimetry. We are currently developing prototype chambers for preradiators at Argonne. (L. Nodulman)

2. Spin Physics at LAMPF

During the period data taking at LAMPF for $\Delta\sigma_L$(np) (E-960) was completed, two Ph.D. theses were finished, and data analysis for E-665/770 (C_{LL}, C_{SS}, C_{LS} for np elastic scattering at T_n ~ 484, 634, 788 MeV and $\theta_{c.m.}$ ~ 50-180°) continued. A paper was published on the construction and operation of the 1m x 3m drift chambers used for E-665/770. Talks were presented by collaborators at the Intersections Between Particle and Nuclear Physics Conference in Rockport, Maine, the International Spin Conference in Minneapolis, Minnesota, and the Santa Fe, New Mexico APS meeting. Argonne physicists presented talks at Santa Fe, CEBAF and the University of Manitoba.

Hardware for the $\Delta\sigma_L$(np) measurements was reinstalled in the neutron beam line after another experiment completed data-taking. All four planes of counters were operational for this running period, whereas only three were instrumented last year. Additional electronics for the third plane fast TDC's and for the fourth plane in coincidence with the third plane were installed and tested. Many scalers were added to record the information from the new electronics. Various improvements in monitoring the bunching fraction and the beam intensity were also made. Data were collected at 580, 650 and a small

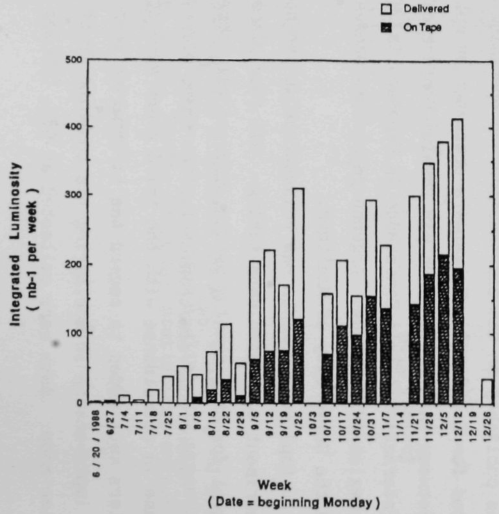

Fig. 16. Fermilab collider luminosity per week delivered and on tape at CDF. At year's end the totals were 3.8 and 1.8 pb^{-1}.

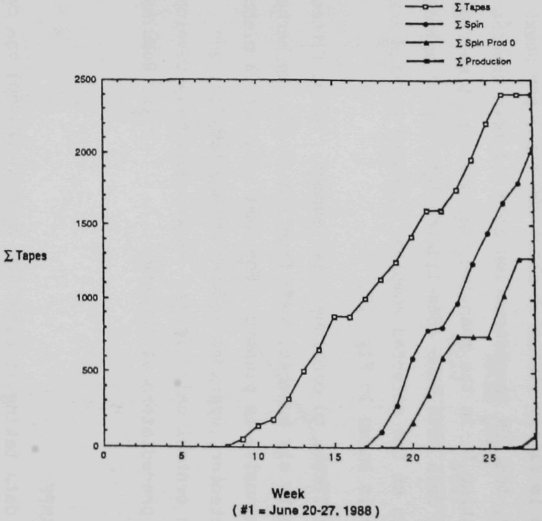

Fig. 17. CDF data tapes produced and processed. Spin selects a small sample, production does reconstruction. For spin this was done on VAXes, for the general sample it is on ACP.

amount at 800 MeV. Data analysis was begun after the end of the run in early October. Bad spills are being identified, and software was developed to look at correlations of $\Delta\sigma_L$ with various scaler ratios. This experiment will be the basis of a Ph.D. thesis for M. Beddo, a student from New Mexico State University.

Data analysis for E-665/770 continued. The 1983 data were completely analyzed and described in a Ph.D. thesis by M. Rawool of New Mexico State University. After the completion of this work, improvements in the data analysis software were made to increase the reconstruction efficiency by about 30%. Argonne physicists will make new DST's of at least some of the 1983 data in preparation for extraction of final results. In addition, a collaborator from Washington State University (G. Tripard) developed a new scheme to find the elastic counts above the quasielastic background. This scheme results in a reduced uncertainty on the spin-spin correlation parameters, C_{LL}, C_{SS}, and C_{SL}. The software to implement this scheme was written jointly by G. Tripard and R. Jeppesen (University of Montana and a faculty visitor at ANL).

Work on the 1984 E-665/770 data also continued. Final calibration constants for the hodoscope timing and the drift chamber delay lines were obtained for a subset of the data. Production of final DST's will begin early in 1989. This work is being performed solely by ANL physicists.

A sizeable fraction of the 1985 data was used as the basis of the Ph.D. thesis for R. Garnett of New Mexico State University, which was completed in October. A short paper is in preparation describing the results. Analysis of the remainder of the 1985 data has begun by ANL physicists.

In addition to the np scattering data, the E-665/770 tapes included deuterons from the $np \rightarrow d\pi^\circ$ reaction. These data are being analyzed by G. Tripard and R. Jeppesen from the 1983 and 1985 DST's. (The 1984 data were at large angles, kinematically forbidden for deuterons from the $np \rightarrow d\pi^\circ$ reaction.) Considerable effort was made to optimize the extraction of the signal from the raw data. Various techniques were tried which relied on the characteristic momentum versus laboratory angle relationship for this reaction.

In addition to the letter being written on the 1985 data, a number of other papers are planned. A long paper describing the apparatus and the 1983 elastic data has been started, as well as a major paper on all the 1985 results. A paper on the $np \rightarrow d\pi^{\circ}$ measurements will also be written. It is hoped that these papers will all be submitted by the end of 1989. In addition, drafts of two papers by our Texas A&M University collaborators on E-589 (forward np elastic polarization at T_n = 790 MeV using much of the E-665/770 apparatus) and E-961 (C_{NN} for np elastic scattering at T_n = 790 MeV) have been written. The E-961 paper should be submitted early in 1989. Additional papers on the 1984 data, an amplitude analysis of all the np elastic data, and a review paper on the LAMPF nucleon-nucleon program are planned for 1990. A number of papers on E-960 will also be written in 1989 and 1990. (H. Spinka)

C. Experiments in Preparation Phase

1. Nucleon Decay

The last half of 1988 saw many improvements in the Soudan 2 experiment: The operating mass was increased from six halfwalls to eight halfwalls (275 tons), completing the first quarter of the detector. (A halfwall is a subassembly of eight 5-ton modules, stacked four across and two high.) The second halfwall, which had a number of dead readout plane sections, was completely rebuilt. The quality of data from the detector was improved with the installation of new anode high-voltage distribution electronics and of the active summer electronics. Recording of data from the active shield was started. The new Exabyte video-tape cassette system was brought into operation, allowing unattended operation of the experiment for many days. Twelve U.S. and eleven U.K. 5-ton modules were delivered to the mine site, giving a total of 85 modules (365 tons) in the underground laboratory at the end of 1988.

The experiment recorded data for 102 days of livetime, with a duty cycle of 58% since the official start of contained-event data taking in July. At the end of the year the total exposure was 4% of a fiducial kiloton year, including data taken with 6, 7, and 8 halfwalls. The contained event analysis used a software filter followed by a physicist scan to identify neutrino interactions. About half of the total exposure had been analyzed at the end of the year, and two candidate neutrino interaction events were found. Both events, which are shown in Figs. 18 and 19, have been tentatively identified as quasi-elastic neutrino scattering, one producing a 200-MeV electron and the other a 140-MeV/c muon. It is noteworthy that the latter event is below threshold for all other operating proton decay detectors. The neutrino event rate we observe is consistent with expectations based on Monte Carlo calculations. About 35% of the active shield, including the entire ceiling, was operational for most of the data set. Both neutrino candidates were well contained with no associated shield hits.

Detector performance was also improved by systematic programs to repair dead and noisy channels, reduce noise pickup, and lower trigger thresholds. The quarter of the detector now in operation has nearly 12,000 preamplifier channels multiplexed onto 4000 ADC's, so this was a substantial effort. In addition, the 64 independent readout plane high voltages were adjusted in several iterations to obtain the same average pulse height from cosmic ray muon tracks. This has substantially improved the uniformity of response of the detector. Finally, new software to deal automatically with high voltage supply trips was brought into operation. Trips of high voltage supplies for readout planes and drift voltages occur a few times per week, and usually can be reset and the voltage run back up without problems. Because this required operator intervention, some running time was lost with part of the detector insensitive. Now most trips are reset immediately and the amount of running time lost has been reduced to a negligible level.

Several improvements in the data acquisition and analysis procedures contributed to the efficient operation of the experiment this quarter. The cluster of VAX computers at the mine was expanded to include a new VAXstation 3200 microcomputer, which now serves most of the user terminals. This allows the VAX 11/750 to be dedicated almost entirely to data acquisition. The two VAXstation 2000 microcomputers are used for data compaction and contained event filtering, which take place automatically at the end of each run. A

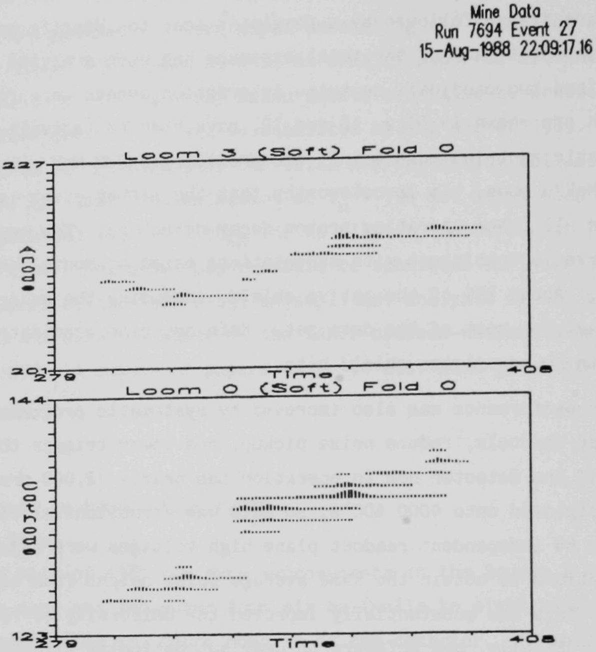

Fig. 18. Two orthogonal views of the first electron-neutrino scattering event found in Soudan 2 data. The anode (top) view of the event represents a region of the detector about 20 cm in the drift direction (horizontal scale) by 35 cm in the anode direction (vertical scale). The cathode (side) view is 20 cm in the drift direction (horizontal scale) by 20 cm in the cathode direction (vertical scale). The irregular topology and multiple hits on many channels identify the event as an electromagnetic shower. The radiation length in the detector material is about 8 cm. This upward-going shower develops from the lower left to the upper right in both views, and has a total energy of about 200 MeV. About 6% of the electron showers observed in the recent test beam calibration of a Soudan 2 module have a similar topology. This event is below trigger threshold for the Frejus detector, the only other large nucleon decay experiment using the tracking-calorimeter technique.

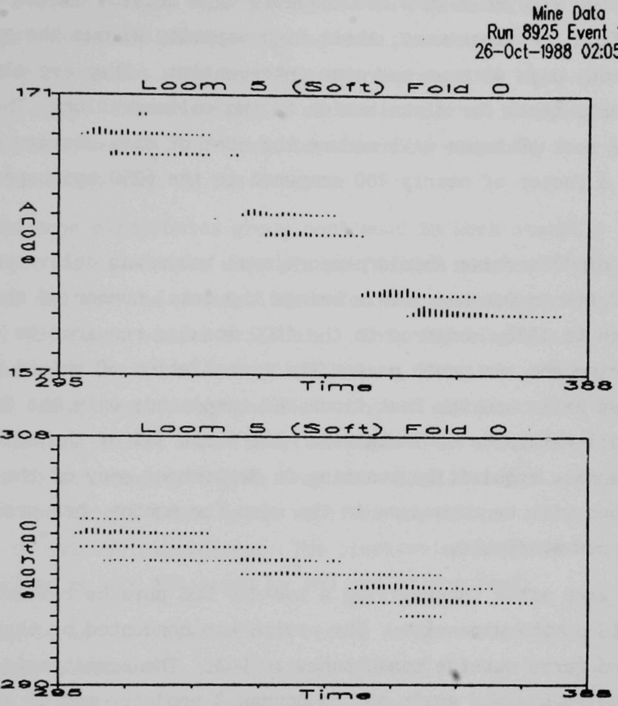

Fig. 19. Two orthogonal views of the first muon-neutrino scattering event found in Soudan 2 data. The track is about 15 cm long, which corresponds to a muon momentum of about 140 MeV/c. The track is identified as a muon because it is approximately straight in both views, with single hits on most channels. The increase of pulse height along the track shows it to be travelling downwards, from the upper left to lower right in both views. The track is probably a μ^- since no decay electron is seen at the end of the track. Stopping μ^- in Soudan 2 are usually captured in iron nuclei and do not decay visibly. Muons of this low energy are below threshold for all other nucleon decay detectors now in operation.

dramatic improvement in the operation of the experiment was achieved with the installation of two Exabyte 8-mm video-cassette tape drives. These are used to record data from the experiment; their high capacity allows the experiment to operate for many days without operator intervention. They are also used to make copies of data tapes for distribution to the collaboration. The high capacity and low cost of tapes will reduce the cost of data storage and distribution by a factor of nearly 100 compared to the 6250 bpi tapes used previously.

A shipment of 176 active shield proportional tubes was delivered to the mine site from Tufts in October. This brings the total number of shield modules at Soudan to 1176, compared to the 1400 modules required to complete the shield. During the six month period the installation of shield modules on the East and West walls and the East floor was completed; only the West floor and the North wall remain to be installed. The first 35% of the shield was used for routine data acquisition starting in September; many of the new wall and floor sections will be turned on in the next few months when preamplifier electronics becomes available.

During the week after Thanksgiving a two-day DOE physics review of Soudan 2 was held at the mine site. The review was conducted by three DOE/HEP staff members and three outside consultants to DOE. The committee's charge was to review the status and goals of the Soudan 2 project, and to assess the impact on physics goals of operation with a 550-ton versus an 1100-ton Soudan 2 detector. At the conclusion of the review the consultants recommended to DOE that the full 1100-ton Soudan 2 detector should be completed as rapidly as possible. The DOE has subsequently decided to accept these recommendations, and a funding plan has been agreed to which will complete construction in 1992.

The Argonne module factory completed the assembly of ten 5-ton module stacks (through Module #67) and ten pairs of readout planes (through Module #65) in the six month period. Four U.S. modules were shipped to the mine, for a total of 54 U.S. modules underground. Module #58 was installed on the module factory cosmic-ray test stand and used to accumulate a sample of throughgoing and stopping muons. The Argonne group devoted a major effort to isolating a clean sample of stopping cosmic-ray muons and to analysis of the pulse height variation along stopping muon tracks. There was good quantitative agreement with the expected increase of ionization as tracks slowed to a stop. Direct analysis of the sample of stopping muon tracks showed that Soudan 2 will be able to determine correctly the direction of 86% of the muons which stop in the detector.

The Argonne electronics group continued to work steadily on a number of important projects. Orders were placed for the remainder of the West side ADC electronics and for the preamplifiers for the second quarter of Soudan 2 as soon as FY1989 funds became available. This ADC electronics fabrication project includes the final lot of ADC cards, Multibus crates, receiver amplifiers, data compactors, and 8086 control electronics. Included in this are eight crates of new anode receiver amplifiers which have two-fold summer front ends to accommodate inputs from both East and West sides of the detector. The single-input anode receiver amplifiers now in use will be converted to cathode amplifiers. The clock-noise suppression modification had been installed on all ADC cards by the end of the year.

Thanks to an intensive effort by the Argonne electronics group, the active summer electronics for the East side of the detector was constructed and installed during July, August, and September. The system consists of 248 cards in 16 crates; each card accepts up to 64 analog signal inputs from anode or cathode preamps, and sums them in groups of 8 onto single outputs, each connected to an ADC channel. This allows a single ADC to digitize signals from up to eight physically separated anode wires or cathode strips. It eliminates reflections and signal distortions which were present in the passive summing scheme used previously, and improves the pulse-height resolution of the detector.

Work proceeded rapidly on the design and prototyping of the cathode edge trigger electronics, culminating in a successful test of a prototype card at the mine. This electronics will be functionally identical to that currently in use for the anode edge trigger, but will be implemented using surface-mount technology and programmable logic devices on small daughter boards mounted directly on the ADC cards. The anode edge trigger now in use is implemented on printed circuit cards in separate crates, requiring much more floor space, electrical power, and cabling than the daughter boards being developed for the cathodes. The cathode edge trigger will operate in conjunction with the anode edge trigger to give higher efficiency for nucleon decay and neutrino events than can be obtained with the anode trigger alone. It is also expected to lower the trigger rate arising from radioactivity, easing the burden on the data acquisition system as the detector is expanded.

During the fall measurements were made of the random hit rate in two special detector modules with non-G10 readout planes, which had been installed back-to-back in the seventh and eighth halfwalls. It has been recognized for some time that the glass component of the G10 readout plane material adds significantly to the level of internal radioactivity in the 5-ton modules. The measurements showed the random hit rate to be about four times lower in the region of the non-G10 planes, giving new impetus to the ongoing program to reduce the amount of G10 in new modules.

Argonne physicists continued to devote a major effort to installation and turnon activities at the Soudan mine site. This included electronics installation and upgrades, electronic noise suppression, module assembly and installation, and work on the gas system. Argonne physicists also contributed substantially to data acquisition operation of the detector, to offline monitoring of detector performance, and to the contained event analysis. After the active summer installation the contained event filter then in use began to reject a larger fraction of the contained events due to an increase in random hits outside the fiducial volume. This was caused by the increased bandwidth of the new electronics and had been predicted. The subsequent rewrite of the filter program at Argonne not only solved this problem but also increased the efficiency for neutrino events and improved the rejection of noise events. This has substantially reduced the physicist scanning load.

During the past year much effort has been devoted to the Monte Carlo calculation of efficiences and background for specific nucleon decay modes for which Soudan 2 has special advantages. This work has been led by a Minnesota graduate student, Steve Werkema, as part of his Ph.D. thesis. It is being performed in collaboration with Gino Saitta at the University of Ferrara in Italy and physicists at Minnesota and Argonne. A major goal was achieved this quarter with the presentation of the detailed results for two decay modes at the DOE review of Soudan 2 in November. These results are summarized in the following table:

Mode	Cuts	Efficiency	Background
$p \to \nu K^+$, $K^+ \to \mu^+ \nu$	loose	32%	0.53 events/kton-yr
$p \to \nu K^+$, $K^+ \to \mu^+ \nu$	tight	10%	0.04 events/kton-yr
$p \to \mu^+ \pi^+ \pi^-$	loose	28%	0.06 events/kton-yr

The efficiencies (acceptances) achieved are similar to those of other experiments, but the neutrino interaction background levels which remain after acceptance cuts in Soudan 2 are five to twenty times lower than in other experiments. Work on the Monte Carlo analysis is continuing to estimate efficiencies and backgrounds in other modes, and to improve the accuracy of the detector response simulation. Monte Carlo events were also used during the quarter to measure the efficiency of contained event filter algorithms, and to train scanners to recognize neutrino events and stopping muons.

During the fall much effort was devoted to obtaining and analyzing 5-ton module calibration data at the ISIS charged-particle test beam at the Rutherford Laboratory. The U.K. Module #31 was installed and brought into operation at the test beam. A total exposure of about 70 hours was obtained using pions, muons, and electrons at four momenta between 170 MeV/c and 400 MeV/c, including both positive and negative beam particles. Data were taken at a variety of angles of incidence of the beam on the module. The data at 236 MeV/c (the momentum of the muon from kaon decay at rest) were analyzed in detail for presentation at the November DOE review. A momentum resolution of

11% was obtained from range measurements of stopping μ^-. Decay electrons were observed for 58% of the stopping μ^+ and 12% of the μ^-, in agreement with expectations from the amount of plastic in the detector. Negative muons which stop in the steel of the detector are expected to be captured before they decay, giving Soudan 2 the ability to distinguish between μ^+ and μ^-. An energy resolution of 21% was found by counting hits for 236-MeV electrons, again in agreement with expectations. The pion data have not yet been analyzed. (D. Ayres)

2. Fermilab Polarized Beam

The major activities in this period included preparations for the next running period, work on the Primakoff and Coulomb-Nuclear analyses (both essentially completed), analyses of the beam performance, and discussions concerning future activities. Figure 20 shows the qualitative relationship. A paper was published in Phys. Rev. Lett., and there were many talks and papers in conference proceedings.

There were six talks from E-581/704 presented at the International Spin Symposium (Minnesota) in October. These were: Overall Summary of E-704 by A. Yokosawa; Primakoff Polarimeter by T. Yoshida; Coulomb-Nuclear Polarimeter by G. Pauletta; $\pi°$ Inclusive by M.Nessi; The E-704 Spin Precession Snake by D. Underwood; and The Fermilab Polarized Beam by F. Luerhing. These will be published in the proceedings along with summary talks by some of the collaborators.

The proceedings of the Symposium on Future Polarization Physics at Fermilab were published and included six papers specifically from E-581/704 and a number of others by collaboration members. There were also many talks relevant to future experiments. Our contributions included Polarized Proton and Antiproton Beams at Fermilab by R. Coleman; Measurement of Beam Polarization by Primakoff Polarimeter by K. Imai; Coulomb Nuclear Interference Polarimeter by A. deLesquen; Polarized Beams from Σ^+ Decay by D. Carey; and Future Plans for the MP Line (Both General and Specific) by D. Underwood. Related experimental reports included: A Long Polarized Target for the

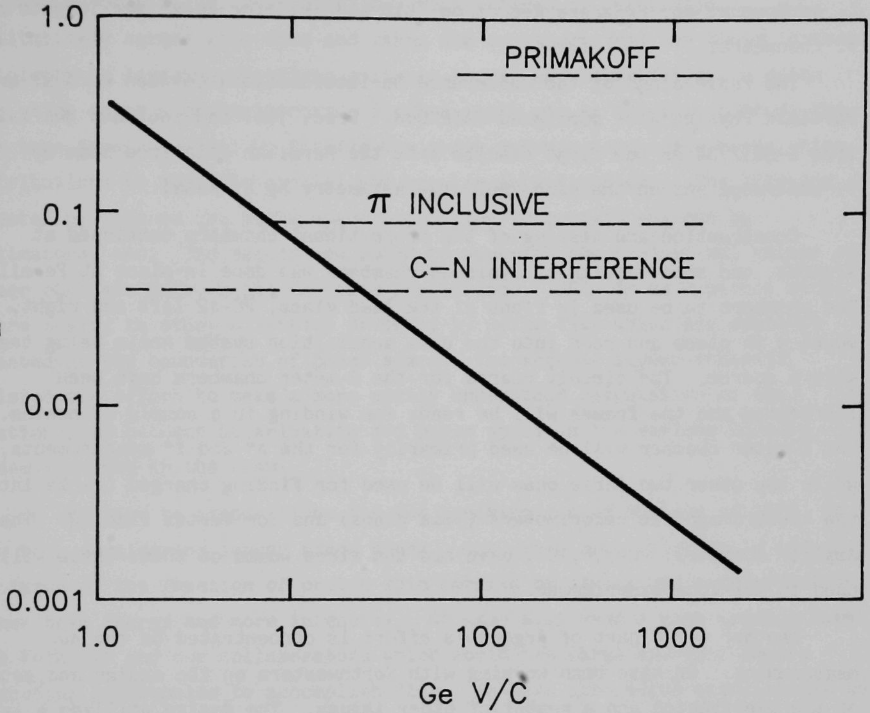

Fig. 20. Qualitative relationship of the energy dependence of conventional polarimeters to the energy dependence of the three new polarimeters used in the E581-704 run earlier this year. The Primakoff, coulomb-nuclear, and pi-inclusive asymmetries have very small energy dependence, while the usual strong interaction interference asymmetry at low t falls rapidly with energy.

Fermilab Muon Beam by H. Spinka; Polarization Physics at CERN and DESY by L. vanRossum; and Progress Report on ^{6}LiD and ^{7}LiH for Polarized Targets by P. Chaumette.

The Proceedings of the Conference on Intersections between Nuclear and Particle Physics were published (AIP Conf. Proc. 176) and included two talks from E-581/704 on the first results from the Fermilab Polarized Beam by D. Underwood and on the pion inclusive asymmetry by M. Nessi.

Construction and testing of the proportional chambers continued at Argonne, and some testing of finished chambers was done in place at Fermilab. The chambers to be used in front of the lead glass, PC-12 left and right, were mounted in place and read into the data acquisition system while being tested with a source. The circuit boards for the 2-meter chambers have been fabricated and the frames will be ready for winding in a couple of months. The 2-meter chamber will be used primarily for the Λ° and Σ° measurements, while the other two large ones will be used for finding charged tracks into the electromagnetic calorimeters (lead glass) and for vertex finding. The smaller chambers, PC-3,4,10', have had the wires wound on them. These will be used in all four experiments.

Another large part of Argonne's effort is concentrated on the $\Delta\sigma_L$ measurement. We have been working with Northwestern on the design and setup of the electronics and a number of other issues. The design utilizes a large number of fast ECL memory units. These will provide a measurement of beam transmission and/or scattering angle for every beam particle at a rate of several megahertz. Scalers will accumulate for each scattering angle for each beam polarization bin, etc.

Argonne is responsible for most of the remaining construction for the polarized target. The target is primarily for $\Delta\sigma_L$ in the coming run, but will be used for test runs of two-spin inclusive measurements which may be the focus of our efforts in the future. The work is progressing well as described in another section.

Many studies have been done of the beam performance, comparing information from data tapes with calculations. One example is the hodoscope encoding efficiency, which is believed to be affected by delta rays locally and perhaps beam halo. A simulation of the effects of delta rays qualitatively agrees with data and leads one to expect that one could increase efficiency by lowering phototube voltages to decrease sensitivity to delta rays which cause encoding errors. Another topic was an attempt to study the beam tune in more detail by fitting the track position and slope correlation distributions to find the spatial and angular magnifications. The fits are affected by cuts on the phase space population in certain regions by collimators, etc. The values are found to approach the theoretical values as looser cuts are made on the particle populations. This is as expected since we are trying to study a lattice property by using fits which are somewhat affected by the boundaries of phase space. The Argonne summer students assisted the effort to make a more easily understood calculation of the relationships between polarization and phase space in the various Lorentz frames involved in the beam.

In addition to preparations for the upcoming run at the end of 1989, we have been considering longer range plans. Any experiment which would address the issue of the fraction of proton spin carried by gluons would benefit from higher beam energy and more intensity. We have discussed a beam upgrade with both Fermilab and our collaborators which would use large aperture super-conducting quadrupoles to accomplish this. We have also begun calculations to see which reactions can best address the gluon spin distribution at particular values of x.

A detailed study of new spin precession snake solutions has found a solution which might be very useful in several accelerators and indicates a new way to tune the spin direction in our beamline. (D. Underwood)

3. ZEUS Detector at HERA

The hadronic and electromagnetic sections of the prototype calorimeter were stacked with clad DU plates and the two sections were mated together during the second half of 1988. The assembly of wavelength shifter and PMT will occur in January of 1989. Good progress was achieved in setting up the cosmic ray stand. Some orders were placed for components of the production modules in preparation for module production startup early in 1989.

Module Assembly (Argonne)

The stacking of the hadronic calorimeter (HAC) section, begun in June, continued through July and several small problems were encountered, the most serious being that the scintillator tiles were cut slightly too large, which required modification to the scintillator alignment jig. The unit cell of the HAC nominally allowed 4.3 mm to accommodate the 2.6 mm thick scintillator and to take up variations in uranium thickness or flatness. By suitable choice of area for the foam spacer above and below each scintillator tile, it was still possible to adjust the scintillator position transversely with a few pounds of force even when the stack was compressed. The spacers were located and glued to the uranium cladding using the scintillator alignment jig. Spacers were available in four heights and, using the data base of uranium plate thickness measurements, the most suitable spacer height was selected to minimize the stack height difference from nominal height. The height of the completed HAC was about 1 mm less than the nominal height and the variation in flatness over the 3 m length was nowhere more than 0.8 mm. No problems were experienced with achieving the required tension in the 26 steel straps used to compress the HAC stack. A hydraulic stud tensioner was used for this purpose. The flatness of the front plate of the HAC calorimeter was generally good to about 0.25 mm except near one end where deviation approached 0.5 mm. This proved not to be a problem in mating the HAC and electromagnetic calorimeter (EMC) sections together later. It is estimated that the HAC assembly time will be about fifteen days for two people.

A separate stacking fixture was built for the EMC section, essentially a three sided box open at the top and on one long side. This is shown in side and end views in the schematics of Figs. 21 and 22, respectively. The stacking was carried out in November.

Quite different problems are encountered in locating spacers in the EMC section, as compared to the HAC section, since there are no slots in the uranium plates. Spacers are of I-beam cross section and run the entire width

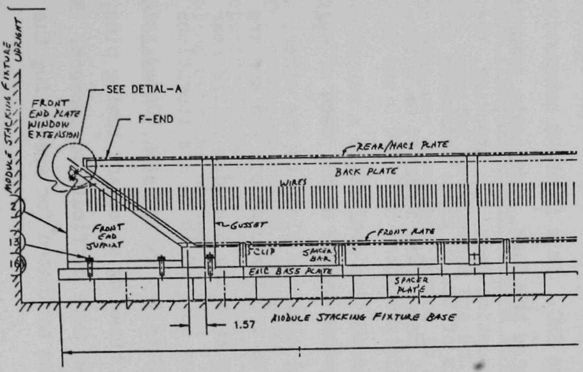

Fig. 21. Front end of EMC stacking fixture as assembled on the bed of the main module stacking fixture.

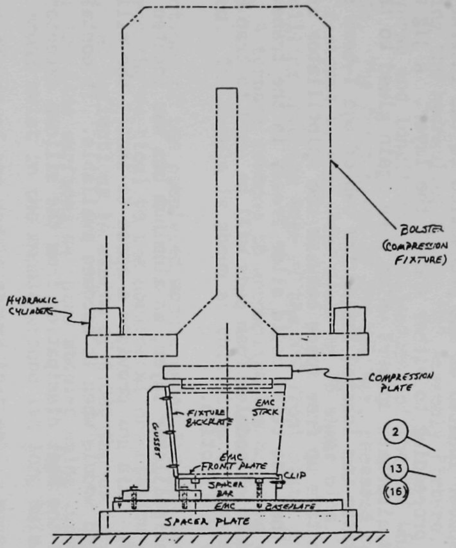

Fig. 22. EMC stack compression using the HAC bolster in order to measure stack height.

of the DU plates. Continuity from a completed layer to the next one was achieved by using the spacer located on the projection to the interaction point as the start for proceeding to either end of the layer. A jig with adjustable bars located alternate spacers which were again glued to the clad DU plate. The scintillator was located inside the web of the I-beam spacers but no foam was used to take up free space between the scintillator and adjacent DU plates, so that the tiles could slide freely in the transverse direction. In the production modules foam pads will be used to trap EMC scintillator, as in the HAC section.

After the fourth scintillator layer, an aluminum box was located followed by the next layer of DU. This box provides a space to insert the silicon pad detector in the completed module when it becomes available. It contains water cooling loops to handle the heat dissipation from the silicon detector electronics.

After completing the stack, the height of the stack, compressed with the nominal loading, was measured. Compression was achieved using the same bolster mechanism as designed for the HAC, which requires much higher compressive loads than does the EMC. This is shown schematically in Fig. 22. While this accomplished the task, a separate compression device will be designed for the module production task. In stacking, the spacer height was again selected on the basis of the DU plate thickness data base and the resulting mean compressed stack height was found to be within 0.03 inches of design height.

The EMC stack is held together by 269 wires, each of which passes from one edge of the rear structural aluminum plate to the other, around the front plate of the stack. These wires are fixed at one end and are tensioned by means of an autoharp tuning pin entering the edge of the rear plate, at the other end. Wires were tensioned to ~ 60 lb in six iterations using the vibration frequency of the wire to set the tension. A small number of problems were experienced with breaking wires and tuning pins, the former easily dealt with but the latter more difficult to correct. Based on this experience a time of 21 days was estimated for assembling the EMC section.

The HAC and EMC sections were mated by lowering the HAC box onto the EMC section using the hydraulics of the HAC assembly fixture, with provision for easy transverse and longitudinal adjustment of the EMC which rested on sliding bearing pads. The front plate of the HAC box, recessed to take the EMC rear plate, was fastened to this rear plate by 76 shear pins. Inserting these pins required drilling into the edge of the HAC front plate which proved to be time consuming. Alternate schemes to accomplish the coupling are being investigated. The module is shown at this stage of assembly in Fig. 23.

Deflections of the completed module under its own weight were measured in rotating from the vertical to the horizontal orientation using optical survey techniques. No deflections in excess of 0.020 inches were observed. The flatness of the side surfaces was also studied using these techniques and revealed a small twist in the module around its long axis. Study of the torsional stiffness of the module showed that only a modest force would be required to rotate one module end plate relative to the other by ~ 1 mm. This may be necessary when installing modules in the spokesplates if the bolt holes are slightly misaligned.

<u>Depleted Uranium Plate Production and Cladding (ANL/Wisconsin)</u>

The 21 DU plates required to assemble the EMC section were clad during September after some problems were experienced in achieving welds of the required strength with the 0.004 inch thick stainless steel used. The solution adopted was to use a 0.001 inch molybdenum foil barrier between the uranium and the steel.

The contract for producing the DU plates for the 32 barrel modules was placed with Manufacturing Sciences Corporation in this reporting period. Plates will be supplied over the period FY 1989 - FY 1990.

Bids for cladding the DU plates with stainless steel sheet were received in November.

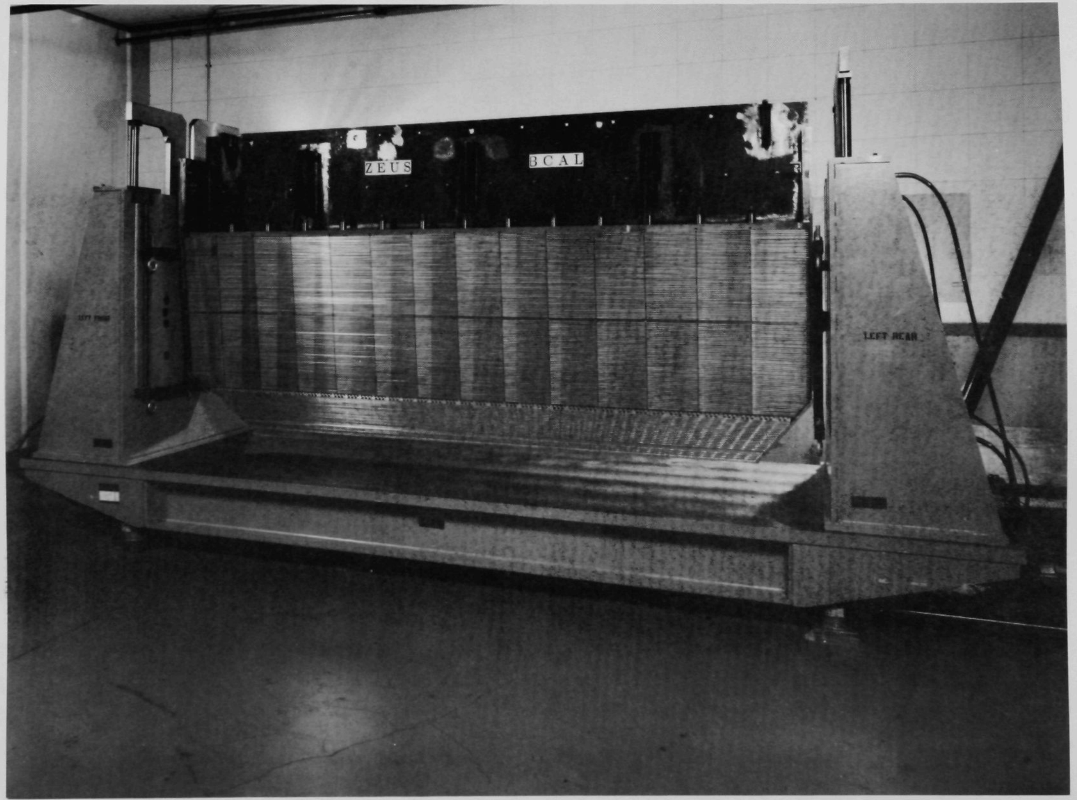

Fig. 23. Prototype BCAL module in stacking fixture after all stacking is completed.

Optical Readout (Ohio State University)

The remaining third of the HAC scintillator and all of the EMC scintillator were delivered to ANL in this period. The HAC wavelength shifter was completed and installed on one side of the prototype module. The remainder, together with the EMC wavelength shifter will be installed in January. The HAC scintillator for the first production module was laser cut and received at OSU in December. It is expected to be all wrapped and mapped by February. Checkout of sizes for the production module EMC scintillator and all the WLS is proceeding preparatory to letting the contract to laser cut these components.

DuPont continued to experience problems in fabricating the encapsulated point ^{60}Co sources to be used in mapping the longitudinal response of calorimeter towers.

Photomultiplier and Magnetic Shields

The so-called holey plates were installed in the back beam of the module and photomultipliers for the HAC wavelength shifter in place were also installed. Several of the components for the production modules were put out for bid. These include the soft iron for PMT shields, the co-netic shields and fabrication of the holey plates.

Electronics

Extensive tests of the prototype electronic readout system were carried out in the November CERN-SPS test beam studies of the FCAL prototype calorimeter. Sufficient supertowers were instrumented for hadronic showers to be measured. On-line analysis of the data revealed no problems but detailed evaluation must await off-line analysis.

Design of the readout system to be used with the calorimeter was begun by Columbia in this reporting period. This system will be available for use in calibrating BCAL modules at Fermilab at the beginning of 1990 and will use the switched capacitor pipeline designed at the Fraunhofer Institute.

Laser Calibration (Pennsylvania State University)

Severe time jitter problems were observed in firing the laser during the tests carried out in July-August. These problems were eventually traced to the spark gap used in firing the laser. Problems were also experienced in monitoring the light output using photodiodes. Alternative monitoring techniques are under study.

Preparations for Production Module Stacking

Agreement was reached with DESY for them to purchase sufficient end plates and back-beams for 32 modules, together with stiffener tubes to assemble 8 dummy modules to be used in the magnetic field mapping of the ZEUS detector. This field mapping is expected to occur in April 1989. Argonne and the University of Manitoba are collaborating to produce a system of Hall-probe-based magnetic field sensors with necessary data acquisition system, to map the field on a coarse grid over the FCAL, RCAL and BCAL regions. These data are important in understanding the response of the scintillator since this is now known to depend on the ambient magnetic field.

Since these HAC boxes will not be released for BCAL module assembly until this field mapping testing is completed, ANL contracted for an additional six module HAC boxes with delivery starting January 1989.

Contracts for the tensioning straps, plate inserts and spacers sufficient for the hadronic sections of the first six BCAL modules were let, with delivery by January 1989. Agreement was reached with Columbia to machine the aluminum extensions of the module end plates in the Nevis Lab shops, with delivery to begin in December.

Uranium plates for the first module will be delivered in January 1989 and plans for cladding the plates for the first few modules at ANL were initiated in this reporting period.

Plans to produce the mechanical components of the EMC section were begun but contracts will not be let until January-February 1989.

These plans are aimed at beginning module assembly of the HAC sections in February 1989.

II. THEORETICAL PROGRAM

Theorists in the high energy physics division have carried out a program of formal and phenomenological research. Topics included are: collider physics phenomenology, production of vector bosons at large transverse momentum, strategies for top quark detection, heavy quark production dynamics, bounds on vector boson couplings, prompt photon production with polarized proton beams, models for spin-weighted parton distributions, a new derivation of the Altarelli-Parisi equation, QCD parton recombination, QCD and Regge theory, new infinite-dimensional algebras and SU(∞), and the chiral Schwinger model. More details of these activities are included below.

Prompt Photon Production with Polarized Proton Beams

Ed Berger and Jianwei Qiu have calculated cross sections for direct photon production at large transverse momentum in proton-proton interactions. In Argonne report ANL-HEP-PR-88-64, submitted to Physical Review, they argue that inclusive direct photon production at large transverse momentum with longitudinally polarized beam and target is an incisive probe of the polarized gluon density in a proton. To help motivate future experiments and assist in their design, they provide predictions of the polarization asymmetry for a range of reasonable choices of the polarized gluon density. The cross sections are small at fixed target energies, but the effort to measure them is necessary if the polarized gluon density $\Delta G(x,Q^2)$ is to be determined. In order to obtain their predictions, Berger and Qiu parametrize spin dependent parton densities and compute their evolution with Q^2. Their densities provide good agreement with the spin dependent structure function $g_1^p(x,Q^2)$ measured in deep inelastic lepton scattering.

New Infinite-Dimensional Algebras and SU(∞)

Infinite dimensional algebras, most of which have been invented by physicists, are maturing as a technical calculational tool for the study of critical phenomena, strings, and super-membranes. A new type of such algebras has been introduced recently by C. Zachos in collaboration with D. Fairlie

(University of Durham, U.K.). Its structure constants are trigonometric, not polynomial, functions of the indices of its generators; but this family still contains all algebras that result out of gauge-fixing membranes on the light-cone as a special limit.

After supersymmetrizing their algebras, Fairlie and Zachos found that these are underlied by the sine bracket of quantum-statistics phase-space, which furnishes an efficient basis-independent formation. Moreover, in an unexpected development, the SU(N) invariant subalgebra of their cyclotomic family turns out to have a well-defined, practicable $N \to \infty$ limit. This then leads to a tractable formulation of SU(∞) for the first time, which results in a picture of SU(∞) gauge theory based on the area-preserving diffeomorphisms of 2-surfaces. This formulation appears promising for carrying out hitherto inaccessible large N calculations of outstanding import in particle physics.

The Chiral Schwinger Model

Geoffrey Bodwin and Eve Kovacs have been investigating whether the chiral Schwinger model proposed by Jackiw and Rajaraman actually leads to a well-defined quantum field theory. In the ordinary Schwinger model (two-dimensional quantum electrodynamics) the gauge field has a vector coupling to the fermion field; in contrast, in the proposal of Jackiw and Rajaraman, the gauge-field--fermion-field coupling is chiral. The chiral gauge symmetry of the model is explicitly broken by the ultraviolet (UV) regulator that is used to define the theory's quantum fluctuations. Usually, in gauge theories, the gauge symmetry is a crucial ingredient in demonstrations of the unitarity and renormalizability of the theory. Nevertheless, Jackiw and Rajaraman argue that their model is both unitary and renormalizable. An essential part of their analysis is the computation the fermionic determinant that arises when one carries out the functional integration over the fermion fields in expressions for the Green's functions of the theory. Jackiw and Rajaraman assert that contributions to the determinant involving more than two vertices on a fermion loop vanish in two dimensions. The vanishing of these higher-order contributions is a rather technical issue, but it is one that is central to the argument that the model leads to a well-defined quantum theory. It is this issue that has been the subject of the work of Bodwin and Kovacs.

Arguments for the vanishing of the higher-order contributions to fermion determinant rely on the chiral symmetry property of these contributions, which is exact only if one can dispense with the UV regulator. In the ordinary Schwinger model, the higher-order contributions can be seen by power counting to be UV convergent. However, in the chiral Schwinger model, owing to the lack of gauge symmetry, the gauge field develops a dynamical mass. Then the complete gauge-field propagator contains terms proportional to $k_\mu k_\nu/k^2$, where k is the gauge-field momentum. These terms lead to UV divergences in the higher-order contributions that contain gauge-field loops, so that one cannot, ab initio, remove the UV regulator. However, Bodwin and Kovacs have been able to show that, because of a variant of the Adler-Bardeen no-renormalization theorem for the axial anomaly, the potentially dangerous UV-divergent contributions actually cancel, and the higher-order contributions do indeed vanish. Hence, their work supports the original conclusions of Jackiw and Rajaraman.

QCD Parton Recombination

Collaborating with Frank E. Close and R. G. Roberts, Jianwei Qiu has been investigating a hitherto neglected sector of perturbative QCD which is normally hidden in conventional hadron analyses but has observable consequences in nuclei. There is a modification to structure functions arising from the fusion of quarks, antiquarks and gluons. Close, Roberts and Qiu derive recombination factors, analogues of familiar splitting functions, and compute the effects of parton fusion on the nuclear structure functions. This mechanism causes the structure functions to extend beyond $x=1$; as $x \to 0$ it provides a source of shadowing within the framework of QCD. They find that the loss of momentum when nucleons bind is shared almost equally between $q\bar{q}$ and gluons. The work predicts that the nuclear modification of the gluon distribution is a significant suppression as $x \to 0$ and enhancement for $x \simeq 0.2$. They point out how hadronic ψ production may be used to disentangle this shadowing mechanism from other nuclear effects.

Bounds on Vector Boson Couplings

In the preprint ANL-HEP-PR-88-97 (to be published in Phys. Rev. D), Chien Peng Yuan has examined the bounds on the non-standard WWV couplings that can be extracted from the existing low energy data, without assuming some couplings are zero. He uses a regularization procedure for loop calculations that gives Lorentz invariant results which therefore do not depend on how integrals are performed. These bounds turn out to be only a little bit better than those given by unitarity requirements. In addition, the work shows how some relations between parameters can be extracted. The work also examines how well the measurements of the W^+W^- cross section at LEP2, and WZ and $W\gamma$ production at hadron colliders, can restrict the values of the anomalous WWV couplings. Yuan finds that significant improvement, with respect to the bounds set from low energy experiments and unitarity, can be achieved at an upgraded Tevatron, at LEP2, and at a 400-GeV e^+e^- collider. Considerably better bounds can also be set from a new experiment at LHC and SSC.

A New Derivation of the Altarelli-Parisi Equation

Collaborating with John C. Collins, Jianwei Qiu studied how the Altarelli-Parisi equations are derived without using $(1-z)_+$ regularization and $\delta(1-z)$ function insertion. He finds that virtual diagrams from renormalization give a negative contribution to parton evolution, and the effect of these virtual diagrams is equivalent to that of some real diagrams with opposite sign. In this new approach, momentum conservation and valence quark number conservation of parton number densities are satisfied automatically. A consistent probabilistic picture of parton evolution inside a hadron is also given.

Heavy Quark Production

Ed Berger prepared invited reviews of heavy quark production for delivery at two major conferences: the XXIV International Conference on High Energy Physics in Munich and the 1988 Annual Meeting of the Division of Particles and Fields in Storrs. These invited reviews are available as Argonne reports ANL-

HEP-CP-88-67 and ANL-HEP-CP-88-68. They include a summary of Berger's computations of the cross sections for charm, bottom, and top quark production in $\bar{p}p$, π^-p, and pp interactions at fixed target and collider energies. The calculations are done through next-to-leading order in QCD perturbation theory. The sensitivity is explored of results to the choices of renormalization/evolution scale, parton densities, Λ_{QCD}, and heavy flavor masses. Comparisons with available data show that good agreement is obtained for reasonable values of charm and bottom quark masses and other parameters. Open issues in the interpretation of results are summarized including the large size of the next-to-leading order contributions, proper definition of the gluon density, the nuclear A-dependence of charm cross sections, the role of final state interactions, and higher twist effects.

Collider Physics Phenomenology

At the 1988 Snowmass Summer Study on High Energy Physics in the 1990's Ed Berger was an active participant in the working group which addressed applications of quantum chromodynamics. Berger's principal contributions included work on production of prompt photons, heavy quarks, and intermediate vector bosons. The report of this working group has been issued as Argonne report ANL-HEP-CP-89-19 (also Berkeley report LBL-26574). The authors treat some current problems associated with the applications of QCD to event rates in high energy collisions. Emphasis is given to the ambiguities and uncertainties that exist in estimates of signals and backgrounds. The production of jets and isolated photons at hadron colliders is examined in some detail. The problems of jet definition are addressed. Some features of the events underlying the hard scattering process are discussed.

QCD and Regge Theory

Alan White's research has focussed on the application of quantum chromodynamics to soft hadronic processes. This led to the preparation and presentation of a paper "The QCD Vacuum at Infinite Momentum" at the Tucson conference on Hadronic Matter in Collision in which he relates the infra-red analysis of Regge behavior in QCD to the "topological confinment" appearing in the Schwinger model. The work suggests that topological confinement may be a necessary bridge between conventional confinement and the parton model at infinite momentum. In QCD it requires additional (perhaps color sextet) quarks to be present.

In addition, he was involved with the preparation and presentation of a set of lectures, at the 1988 Stefan Banach Institute, entitled "Multi-Regge Theory and the Infra-Red Analysis of QCD". These lectures contain a general review of analyticity properties of multiparticle S-Matrix elements, the related general Multi-Regge theory and the study of the Pomeron in QCD.

Research on these subjects continues and involves a comprehensive review to be entitled "Analytic Multi-Regge Theory and the Pomeron in QCD".

Strategies for Detection of the Top Quark

Ed Berger, C.-P. Yuan, visitor Frank Paige, and students D. Kuebel and M. Pundurs have been examining prospects for observing top quarks in proton-antiproton interactions at collider energies. Focussing on values of $m_t < m_W$ and on semi-leptonic decay modes, they have calculated expected event topologies associated with both the signal and important backgrounds from bottom and charm quark production. As part of this study, they are assessing the extent to which the ISAJET and PAPAGENO Monte Carlo simulation programs properly incorporate next-to-leading order contributions in QCD. These contributions are especially relevant for production of bottom and charm quarks at large values of transverse momentum. Among the distributions, correlations, and selections being examined to provide evidence for a signal are those in transverse momentum of decay leptons, lepton isolation, two- and three-body transverse mass, and jet multiplicity.

Production of Vector Bosons at High Transverse Momentum

With W and Z bosons being produced at the Tevatron, there is some urgency to understanding their production as well as possible in the context of the standard model. The transverse momentum (p_T) distribution of single W and Z production provides a useful test of the standard model, a possible means of measuring α_s, and a background to new physics. M. Hall Reno (of Fermilab and the C.I.E.A. in Mexico) and Peter Arnold have completed the calculation of the high-p_T production rate to second order in QCD. Previous such calculations, which were concerned with CERN energies, focused on quark-antiquark annihilation and scattering as a source for W's and Z's and ignored quark-gluon scattering. Quark-gluon scattering cannot be neglected at Tevatron energies, where it is as significant as the other mechanism. They have derived analytic expression for the parton cross-sections $d\sigma/dq_T{}^2dy$ for all processes and then integrated these numerically with the proton structure functions. The transverse momentum distribution, normalized by the total cross-section, is shown in Fig. 24.

Models for Spin-Weighted Parton Distributions

Jianwei Qiu, Gordon Ramsey (Loyola) David Richards and Dennis Sivers have formulated models for the spin-weighted quark and gluon distributions in a longitudinally polarized proton. These models embody different underlying concepts concerning the application of spin-dependent forces in the nonperturbative regime of chromodynamics. The different spin densities are used to investigate a possible long-range experimental program using polarized protons.

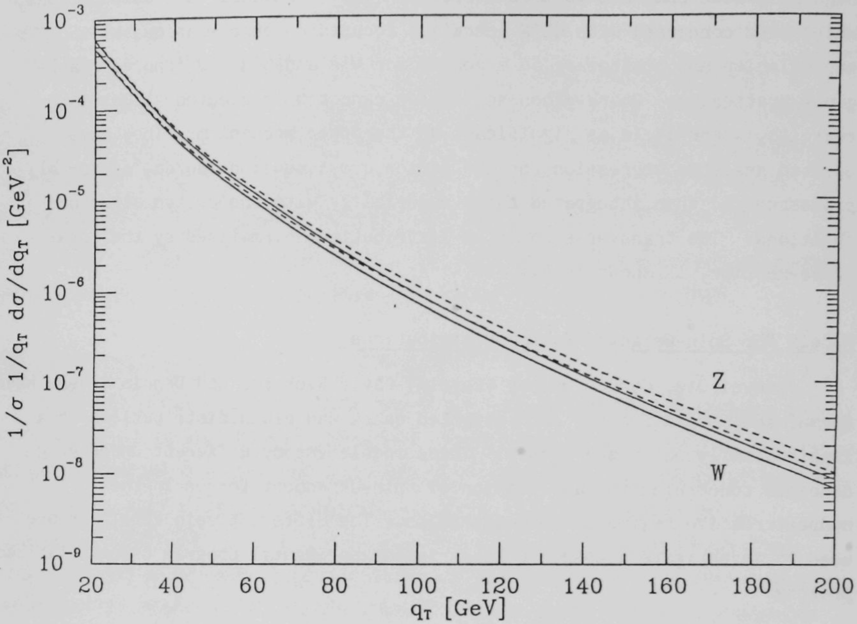

Fig. 24. W (solid) and Z (dashed) production at $\sqrt{s}$ = 1.8 GeV. Normalizing cross-sections are σW^+ = 9.6 nb, $\sigma(Z)$ = 6.1 nb. In each case, the error estimate is delineated by the two lines. This is not a conservative error estimate.

III. EXPERIMENTAL FACILITIES RESEARCH

A. Mechanical Support

Proton Decay

The module construction schedule was maintained at a level of two modules/month during this period.

Polystyrene Inserts - A new vendor was found and encouraged to produce polystyrene inserts. These inserts were produced on new tooling and a special shearing die was built which produces a much cleaner edge perpendicular to the corrugations. This has resulted in inserts which are cheaper and more uniform.

Stacking Fixture - Some improvements have been made in the module stacking fixture to improve the straightness of the modules.

Radiation Levels - An extensive investigation and testing program has been initiated to reduce the levels of intrinsic radiation in both the steel and the materials used to construct cathode boards for the module wire planes.

ZEUS Detector at HERA

The prototype module was stacked in Building 366 and changes were incorporated to facilitate mounting of the electronics and light guides. The prototype electromagnetic calorimeter was also stacked using new stacking fixtures designed during this period.

Cosmic Ray Test Stand - The stands and counters for the cosmic ray testing of the BCAL modules were designed, built, and assembled in preparation for receiving the prototype module.

Module Frames - A contract was awarded to Alumni Tool for fabrication of six module frames to be assembled during FY 1989. A contract was also awarded to Hans Schlack of Osnabruk, West Germany, for fabrication of dummy module frames and the T-beams and end plates for 24 additional modules. This will provide the 32 T-beams and end plates for the magnetic field mapping at DESY. The six modules fabricated in the U.S. will allow the stacking of complete modules to proceed in parallel with the assembly and magnetic field mapping of a dummy assembly at DESY.

Module Installation - In collaboration with University of Wisconsin Physical Sciences Laboratory (PSL) engineers we are developing the techniques and handling devices to install both the dummy and the full size modules at DESY. The handling fixtures will be designed and built by PSL and the alignment techniques and fixtures will be designed and built by Argonne. The adjustable lifting device to be used to install modules is shown in Fig. 25.

Collider Detector at Fermilab

Research and development are proceeding toward the design of preradiators for the electromagnetic shower counters for the barrel calorimeter wedges. These are to be installed during the fixed target run at Fermilab in preparation for the next collider run.

Polarized Beam

Helium-3 System - The dilution refrigerator and superconducting solenoid from Saclay were delivered to Fermilab. The dilution refrigerator was mounted. Assembly of the emergency pumping system (DC powered) was started. Molecular sieve and charcoal traps were completed and installed.

Liquid Helium Dewars - New ASME-code dewars were received and installed. Insert assemblies were designed for all three dewars.

S.C. Solenoid - The solenoid and power supply were installed and tested. The field was measured for uniformity.

Microwave System - The power supply and cooling system were repaired and tested. A mounting table was constructed to hold the system.

Instrumentation - Market searches were made for a helium leak detector and a residual gas analyzer (RGA). Both have been purchased.

Multiwire Proportional Chamber Construction - PC12 left and right have been entirely completed, tested in place, and are ready to be mounted in their respective locations at Fermilab. PC3 has been been assembled, surveyed and bench-tested. PC4 and PC10 prime have been assembled and surveyed. PC8 and PC9 have all their printed circuit boards fabricated and are ready to be mounted on their respective frames.

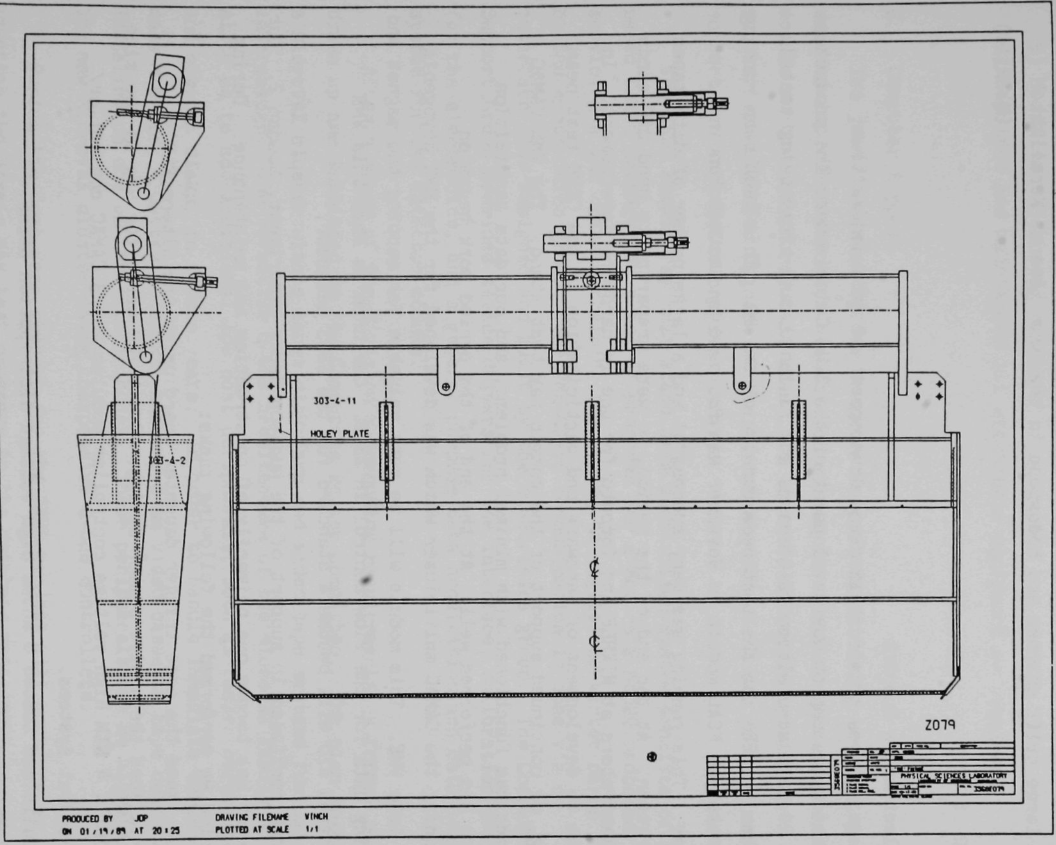

Fig. 25. Adjustable lifting device to be used for installation of ZEUS BCAL modules.

Sketches were completed for a design of a support system to hold PC8, PC9, a large drift chamber and hodoscope in the beam line at Fermilab.

(N. Hill)

B. Electronics Support

A major area of effort involved development of data acquisition electronics to support our development of the ZEUS Calorimeter. The production run of 20 data acquisition (DAQ) cards was finished, and after being tested, was taken to CERN for the test beam running at the PS. This test beam running of a prototype FCAL module in November was followed by another run in December. This running was very successful and a large number of data tapes were written. At the end of the period, we were preparing to send DAQ cards to collaborators at NIKHEF and Toronto for use in hardware development. In addition to development of hardware and participation in the CERN test beam running, we continued support of the cosmic ray test stand. The VME/CAMAC interface has functioned with minimal problems, and our data acquisition hardware has performed well. At the end of the period work began on redesigning the CAMAC multiplexer which was developed for the HRS cryogenic system into VME. This module will be very valuable for mapping the magnet and acquiring data for the slow control in ZEUS. Our hope is that this VME multiplexed A/D will become a standard for the ZEUS detector.

Work continued in support of the nucleon decay experiment, Soudan 2. Our involvment has become one primarily of construction and maintenance. During the period we performed the following tasks:

1) Designed the edge trigger daughter board using the Altera PLD's.
2) Finished the active summer design. Built 280 cards for use in the mine.
3) Built 4 NIM high voltage controller modules and 3 CAMAC controller/ readout systems.
4) Built and tested 8 anode high voltage distribution boxes.
5) Built and tested 20 fan units for the mine.
6) Built and tested 64 preamp assemblies.
7) Modified 50 calibration pulser modules.

8) Modified 40 calibration cards.
9) Modified 125 analog cards.
10) Repaired and maintained all electronic equipment as required.

(J. Dawson)

C. Computer Support

The jobs completed by the Computer Support Group during the past year were to implement the data acquisition system for the ZEUS barrel calorimeter module on the cosmic ray test stand, to lead the effort in writing an acquisition plan for upgrade of the Division's computers and to continue support for a division program library.

The ZEUS cosmic ray test stand data acquisition system consists of a VAX-based CAMAC package and a set of programs for a Motorola 68020 processor servicing a VME crate containing the analog-to-digital converter cards built by the electronics group. The VME-CAMAC communication is done via an interface also designed and built by the electronics group. The Computer Support Group provided device drivers for the interface, calibration programs for the electronics, and a general purpose data acquisition and data logging system for the detector module.

After a study of the Division's computing requirements, a formal plan was drawn up and submitted to the Computing Policy Committee. The plan specifies a MicroVAX cluster with a large disk farm and video tape systems for data interchange. The versatile Q-bus architecture of the MicroVAX family will allow us to add additional low cost peripherals, such as faster cartridge tape and optical disks, in future years. In order to handle immediate demands for mass storage, 4 Gbytes of disks, and two 8 mm video cassette tape units were installed on one of the cluster nodes. These peripherals can be migrated to the new MicroVAX cluster using inexpensive Q-bus controllers.

During the next year support for the ZEUS project will continue by adapting the cosmic ray test programs to the database management system chosen by the collaboration so that the data are consistent with that taken at the FNAL test beam and DESY. The new MicroVAX cluster should be installed in late summer.

(J. Schlereth)

D. Polarized Target Development

^{3}He Recirculation System

The dilution refrigerator and solenoid from Saclay were delivered to Fermilab. The DR was mounted. Assembly of the emergency pump system was started. The last two gas clean-up devices were completed and plumbed.

Liquid Helium Dewars

The ASME-code replacement dewar for solenoid service arrived at Fermilab and was placed in position. Designs for the insert assemblies were completed for all three dewars.

Solenoid

The Solenoid and its power supply were installed. Plumbing and instrumentation were assembled for a test. The magnet was cooled down in a couple of days' time and was tested for performance and safety aspects. The field uniformity of the magnet was measured with NMR and found to be the same as it was before shipment from Saclay. The new power supply also performed well. Some controlled quenches were induced at the request of Fermilab. After the test, work continued on the final power supply instrumentation.

Mircrowave System

The power supply for the microwave source was repaired and tested. The water circulator for the source was repaired and installed. A table for the microwave components was made and the system layout was completed and tested.

Special Instruments

Market searches were undertaken for a mass spectrometer leak detector, a digital radio frequency source for NMR, a small control and status computer, and a residual gas analyzer. A leak detector and a RGA were purchased.

Safety

Several reviews by the Fermilab Cryo Safety group took place during this period. We wrote pressure safety analyses for the three dewars and the solenoid, and obtained final approval for these items. Pressure safety of the ^{3}He recirculation system was extensively discussed and a formal analysis was started.

Miscellaneous

Special polarized target material was prepared at Argonne for use at Brookhaven, as a service to the University of Michigan.

We traveled to Los Alamos to help prepare their polarized target for the E-960 run.

We gave presentations at the Minnesota conference on the status of the Fermilab target, and on our experiments with target material for polarized ^{19}F nuclei. We also wrote up the latter work for publication.

(D. Hill)

IV. ACCELERATOR RESEARCH AND DEVELOPMENT

A. Observation of Nonlinear Plasma Wake Fields

Nonlinear plasma waves were observed in data taken at the Advanced Accelerator Test Facility (AATF) in a July experiment. This came as a surprise because the available drive pulse intensity was considered inadequate to excite a plasma wake field of sufficient amplitude to become nonlinear. Nevertheless, the experimental evidence was convincing and an explanation was discovered.

Figure 26 shows part of a longitudinal wake field scan in which the wake potentials have a distinct triangular wave form characteristic of nonlinear plasma waves. Figure 27 is a scan segment during which the drive pulse charge was changed from 2.9 nC to 4.0 nC. Concurrent with this change was a transition of wave form from near symmetric to near triangular. The amplitude of the wake also increased disproportionately greater than the drive pulse charge. Figure 28 shows a Fourier analysis of a longitudinal wake potential. One dimensional nonrelativistic theory of nonlinear plasma waves predicts that the relative amplitude of the first harmonic to that of the fundamental is a measure of the wave electron density amplitude relative to the ambient density. For these measurements this ratio is about 0.3.

The explanation for these unexpected observations is now believed to be that the drive beam pulse experiences sufficient self-pinch to increase the local beam density sufficient to excite nonlinear waves. Analytical and numerical simulations indicate that the beam pinched to a diameter roughly a third that which it would have without the presence of the plasma.

These conclusions are important for plasma wake field acceleration (enhanced wake fields), for plasma focussing (the same mechanism is in effect), and for basic plasma physics (where there is insufficient theory to explain many of the observed properties).

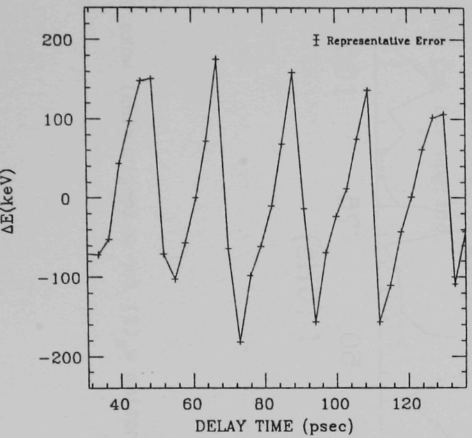

Fig. 26. Longitudinal wake field scan, with plasma density of $n_o = 2.8 \times 10^{13} cm^{-3}$.

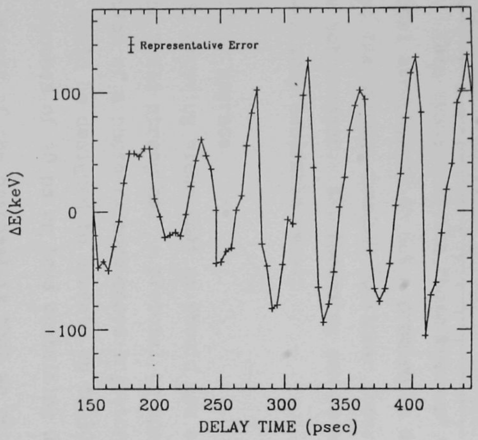

Fig. 27. Longitudinal wake field for the same scan as Fig. 26, with a different delay range. Below 250 psec in delay, the driving beam charge is 2.9 nC. Between 250 and 280 the charge is raised to 4 nC, where it remains for the rest of the scan. The disproportionate rise in the wakefield amplitude is attributable to stronger self-pinching of the driver beam.

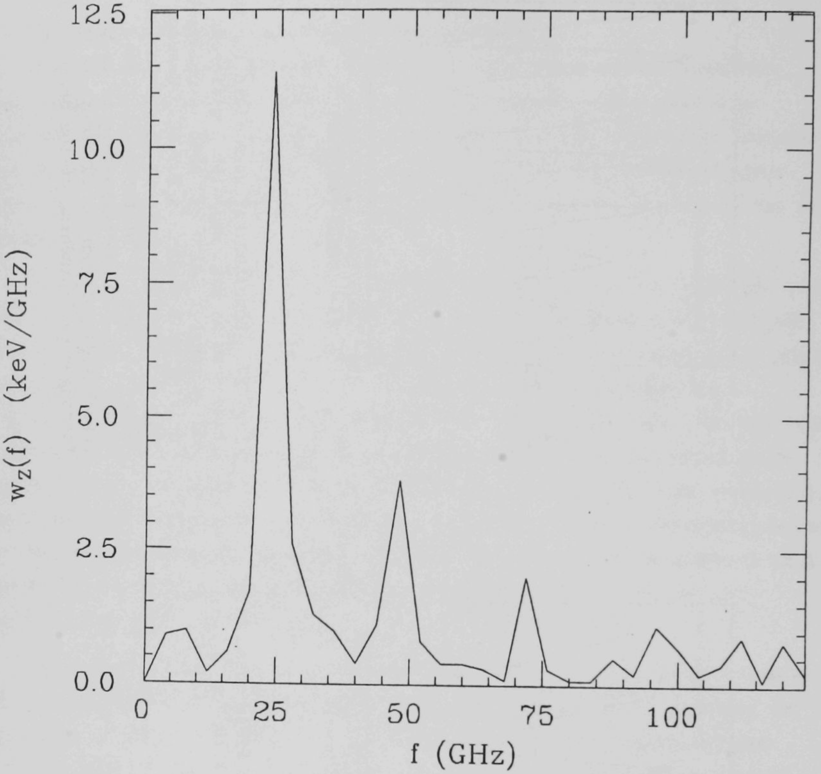

Fig. 28. FFT amplitude function $w_z(f)$ for a longitudinal wake field.

B. Dielectric Wake Field Devices

We now conclude from theory that linear dielectric tube structure wakes are such that the transverse forces on particles in them are proportional to $1/\text{gamma}^2$. This means that the "beam breakup" mode, a serious problem in conventional structures, is not a problem in dielectric wake field devices. Similarly, the strong, usually nonlinear focussing forces found in plasma wakes are not present. All focussing can be accomplished using external elements--a very desirable result.

C. Facility Upgrade

It is becoming clear that we should now extend our wake field experiments to greater field strengths. A proposal to upgrade the CHM electron linac by the addition of a photo-cathode-based injector has been developed. The injector would be designed to operate up to 30 pps, and generate single electron bunches of 10 ps or less containing up to 100 nC of charge.

The spirit of the proposal is that we not become imbedded in laser R&D or in exotic cathode development. Because the emittance requirements are not demanding in our application, the proposed beam brightness is less than that required of projects already underway at other laboratories. In fact, we plan to draw heavily upon the designs developed at these other projects in order to minimize R&D for the upgrade. (J. Simpson)

V. SSC DETECTOR RESEARCH AND DEVELOPMENT

A. Detector Simulation

Development continued on a version of the GEANT detector simulation program for use in designing detectors for the SSC. The principal areas of work were the addition of parametrization of showers to GEANT and improvement of the user interface, particularly in the area of a more flexible system for specification of the detector geometry and properties.

The surface integration technique for integrating energy deposition in calorimeter readout cells was developed and tested with approximate energy density functions. The algorithm treats energy deposition density in analogy to electric charge and performs a surface integration on the boundaries of the calorimeter cell to determine the total energy deposited in the cell. Timing studies continued to suggest about a factor of 50 improvement compared to the full shower simulation in GEANT.

The initial implementation of the subroutine set for streamlining detector specification was completed and used to specify a simple version of a 4 pi SSC detector. That detector specification was being debugged at the end of the reporting period. The detector specification system will next be used to form a version of the Large Solenoid Detector from the 1987 Berkeley summer study. Study of fancier detector specification possibilities such as a detector specification language continued at a low level.

Two physicists were hired to work on the detector simulation project; P. K. Job joined the project in November 1988, from the KFA Juelich Laboratory, and Hans-Jochen Trost arrived in January from Fermilab, where he had been working for the Max Planck Institut in Munich.

The Snowmass '88 summer study was held during this period. Calculations were made there to simulate various detector components. L. Price talked at the Detector R&D workshop held during Snowmass, reviewing the status of detector simulation development that may be of use for SSC detector design.

(L. Price)

B. Radhard VLSI Electronics

During the period a proposal was made to DOE for the development of radiation-hard VLSI electronics for SSC detectors. At the end of the period the proposal was approved and the funding was authorized. In this work we will have collaborators from Brookhaven and Vanderbilt and will interact strongly with an industrial participant. Interaction rates, segmentation, and the radiation environment dictate that front-end electronics of SSC calorimeters must be implemented in the form of highly integrated, radhard, analog, low-noise, VLSI custom monolithic devices. Important considerations are power dissipation, choice of functions integrated on the front-end chips, and cabling requirements. An extensive level of expertise in radhard electronics exists within the industrial community, and a primary objective of this work is to bring that expertise to bear on the problems of SSC detector design. Radiation hardness measurements and requirements, as well as calorimeter design, will be primarily the responsibility of Argonne, Brookhaven, and Vanderbilt. Radhard VLSI design and fabrication will be primarily the industrial participant's responsibility. The rapid-cycling synchrotron at Argonne will be used for radiation damage studies involving response to neutrons and charged particles, while damage from gammas will be investigated at Brookhaven. The Central Design Group has undertaken studies of radiation levels in the SSC interaction regions, and the results of these studies are summarized in a detailed report. The predicted radiation levels require that detector electronics be radiation hard in order that it may operated satisfactorily for a reasonable lifetime. In general, builders of previous high energy physics detectors have not been forced to deal with the problems of radiation hardness in the electronics. Accordingly, the difficulties posed by the SSC bring a new dimension to detector design. The guidelines for this development effort are as follows:

1) The development efforts will be focused on the calorimeter electronics. Argonne has long experience in calorimeter design, construction, and use as evidenced by the calorimeters for the HRS, CDF, ZEUS, and other detectors.

2) The work will focus upon the electronics needed for liquid argon or warm liquid drifting calorimeters as stated above.
3) This project will include extensive radiation damage studies as well as VLSI device and process development. The two areas of work will proceed jointly, in close coordination. Radiation damage exposures and evaluation will be primarily Argonne's responsibility, while radhard device design and fabrication will be primarily the industrial participant's responsibility.
4) No effort will be expended on developing non-radhard devices or designs. An adequate level of radhard expertise exists so that radhard devices will be used at the outset.
5) We will proceed by characterizing the radiation environment in which the electronics must operate, selecting a currently operating radhard process capable of yielding devices which are adequately radhard, and proceeding with a radhard design in that process.
6) The rapid-cycling synchrotron of the Intense Pulsed Neutron Source (IPNS) at Argonne produces 400-MeV protons and a neutron fluence of 10^{12}/sec/sq-cm from the spallation target. This Argonne facility, together with a gamma source such as the source at Brookhaven, will be used for the radiation damage studies. These studies will be done both at 25°C and at liquid argon temperatures. Small prototype calorimeter sections will be operated in the radiation environment.

The objective of this development effort is to design a prototype VLSI version of the SSC calorimeter electronics using a specific radhard process. A phase 2 follow-on project would involve a prototype production run of a number of wafers. Developing this design will require that radiation damage studies have been conducted on devices from the designated process, that devices from the designated process have been run in prototype calorimeter sections in appropriate radiation environments, and that the radhard electronics design is compatible with the calorimeter physics requirements. As discussed above, technologies exist that meet our radiation hardness requirements for neutron and charged particle total dose. The calculations indicate that the gamma-ray levels experienced by the electronics in very forward locations poses a very difficult challenge that cannot be met with current CMOS technology.

(J. Dawson)

C. Superconducting Strip Detector R&D

During the last half of 1988, studies were performed on the detection of 6-keV X-rays using thin film niobium strips fabricated at the National Institute for Standards and Technology (NIST) in Boulder, Colorado. Scanning electron micrograph cross sectional profiles of the niobium strips made at the institute in March showed that the technique of plasma etching resulted in triangular-shaped strips. This was a result of the isotropic nature of a plasma etch in which the plasma undercuts the pattern in the photoresist layer over the niobium. This problem was overcome by subjecting the patterned niobium films to a reactive ion etch. New niobium thin film strips were fabricated in October using a reactive ion etcher at the NIST. Subsequent inspection with a scanning electron microscope indicated the strips now had a more nearly rectangular cross section. Both geometrical types were exposed to 6 keV X-rays from an ^{55}Fe source to observe superconducting-to-normal switching produced by heating after the absorption of an X-ray. The energy deposited in the film by this X-ray absorption is about five times that expected from passage of a minimum ionizing particle through the film. The switching process occurs as follows. The strip is biased at a current very near the superconducting critical current I_c. Absorption of a 6-keV X-ray by the L-shell of a niobium atom produces a photoelectron of approximately 3.4-keV energy and an L-shell hole which creates with very high probability, a 1.9-keV Auger electron during de-excitation. Both electrons quickly range out in the film and deposit all of their energy in the film. On the time scale of picoseconds the ionization energy comes into equilibrium with the lattice, producing a region of temperature much higher than the superconducting critical temperature, T_c. Because the range of the electrons is on the order of 0.05 μm, the normal region thus produced can be approximated as a sphere. This spherical normal region is effectively removed from the cross sectional area of the film, increasing the current density in the remaining superconductor above the critical current density and, thus, producing a normal region in the entire film cross section.

The detection efficiency of X-rays as a function of the ratio of bias current, I, to critical current, I_c, is shown in Fig. 29. Since the number of X-rays traversing the film is not directly measured, the detection efficiency is calculated using the known solid angle subtended by the strip, the known activity of the source, and the measured switching rate in the strip. The threshold value of I/I_c at which switching begins can be used to estimate the radius of the initial spherical normal region produced in the film via the relation,

$$I/I_c = (wt - \pi r_o^2)/wt$$

at threshold. Here, w is the film width, t is the film thickness, and r_o is the hot spot radius. The effective normal region radii for the three samples in Fig. 29 are all approximately 0.1 μm. Using a simple heat balance model and measured values of specific heat of niobium, a radius of 0.17 μm is predicted. This is a factor of two larger than that actually observed. The disagreement indicates the need for a more detailed analytic calculation of the heat dispersion in the film.

Because of the high normal state resistivity of the niobium films, joule heating in the produced normal region causes the region to propagate to the ends of the film. A thermal propagation model developed by our collaborators in the ANL Material Science Division reproduces the observed propagation without any adjustable parameters. Figure 30 shows the measured current and voltage during the switching process. Figure 31 shows the time behavior predicted by the thermal propagation model. Good agreement between the two is evident.

We are currently attempting to improve the sensitivity of strips to small energy deposits characteristic to minimum ionizing particles. To this end, we will begin study of switching in aluminum films with a critical temperature

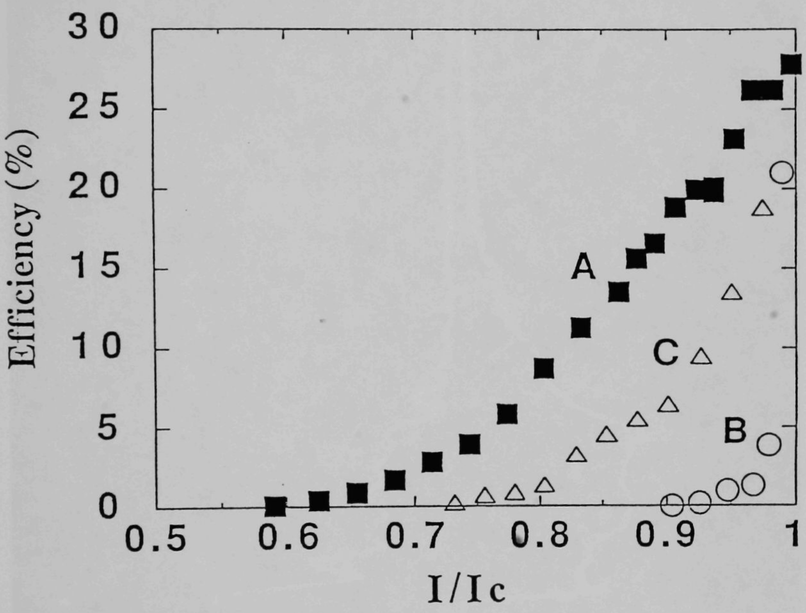

Fig. 29. Switching efficiency as a function of bias current for three Nb detectors tested with ^{55}Fe X-rays. Detectors A and B have a triangular cross section. Detector C has a rectangular cross section.

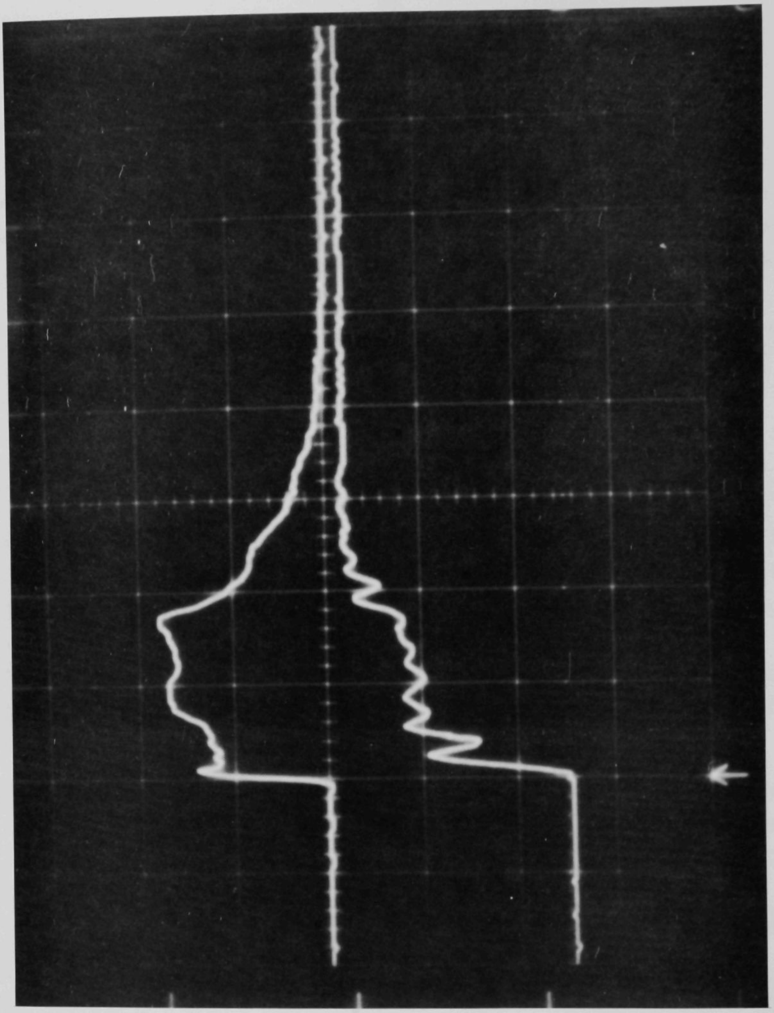

Fig. 30. Digital oscilloscope traces of the voltage (upper trace) and current (lower trace) for switching in detector A from Fig. 29. Middle horizontal line is zero for both current and voltage. The scales are per large division: voltage 0.5 V, current 10 mA, and time 0.2 μs. The bias supply reduces the current to near zero starting at 0.4 μs when a switching event is detected.

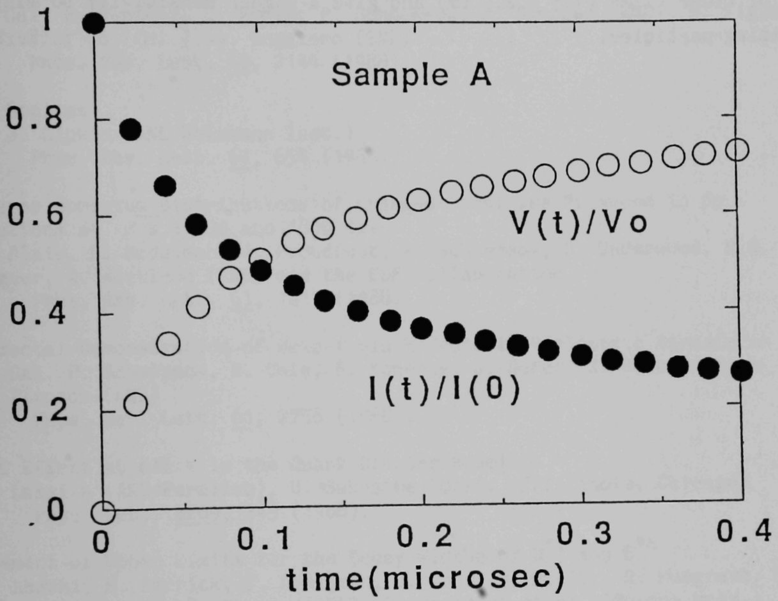

Fig. 31. Calculated time dependence of the current and voltage using a thermal propagation model developed by our collaborators in the Materials Science Division.

near 1K. Such films provide both the advantage of a much smaller specific heat than niobium with a T_c of 9K, and the ability to operate with a bath temperature very near the critical temperature. The combination should allow use of wider films (1.5 - 2.0 μm) and give a higher sensitivity to minimum ionizing particles. (R. Wagner)

VI. PUBLICATIONS

A. Journal Publications, Conference Proceedings, Books

Direct Measurement of Beam-induced Fields in Accelerating Structures
W. Gai, R. Konecny, J. Norem, P. Schoessow, J. Simpson (ANL), H. Figueroa (Univ. of So. Cal.), A. Ruggiero (BNL)
Phys. Rev. Lett. 60, 2144 (1988).

Lipkin Replies
H. J. Lipkin (ANL/Weizmann Inst.)
Phys. Rev. Lett. 61, 654 (1988).

Transverse Momentum Distributions of Charged Particles Produced in $\bar{p}p$ Interactions at $\sqrt{s}$ = 630 and 1800 GeV
R. Blair, L. Nodulman, J. Proudfoot, P. Schoessow, D. Underwood, R.G. Wagner, A. Wicklund (ANL) and the CDF Collaboration
Phys. Rev. Lett. 61, 1819 (1988).

Experimental Demonstration of Wake-field Effects in Dielectric Structures
W. Gai, P. Schoessow, B. Cole, R. Konecny, J. Norem, J. Rosenzweig, J. Simpson (ANL)
Phys. Rev. Lett. 61, 2756 (1988).

The EMC Effect at all x in the Quark Cluster Model
K. Lassila (ANL/Fermilab), U. Sukhatme (Univ. of Illinois, Chicago)
Phys. Lett. B209, 343 (1988).

Measurement of Upper Limits for the Decay Widths of D^{*+} and D^{*o}
S. Abachi, M. Derrick, P. Kooijman, J. Loos, D. Miller, B. Musgrave, L. Price, J. Repond, K. Sugano (ANL), P. Baringer et al. (Purdue Univ.), D. Blockus et al. (Indiana Univ), C. Akerlof et al. (Univ. of Michigan)
Phys. Lett. B212, 533 (1988).

Flavor Symmetry, EMC Results and the Spin Content of the Proton
H. J. Lipkin (ANL)
Phys. Lett. B214, 429 (1988).

Trapping, Thermal Effects, and Wave Breaking in the Nonlinear Plasma Wakefield Accelerator
J. Rosenzweig (ANL)
Phys. Rev. A38, 3634 (1988).

The Equivalence of Dirac-Kahler and Staggered Lattice Fermions in Two Dimensions
G. Bodwin (ANL), E. Kovacs (Univ. of Illinois, Chicago)
Phys. Rev. D38, 1206 (1988).

Finite Temperature QCD with Intermediate - Large Quark Masses
D. Sinclair, J. Kogut (ANL)
Phys. Rev. D39, 636 (1989).

The Phase Structure of the Non-Compact Abelian Higgs Model
J. Oliensis (ANL), P. Suranyi (Univ. of Cincinnati)
Nucl. Phys. B300, 159 (1988).

Construction and Performance of a Large Area Liquid Scintillator Cosmic Ray Anticoincidence Detector
J. Napolitano, S. Freedman, G. Garvey, M. Green, K. Lesko, J. Nelson, J. Worthingtron (ANL/PHY); K. Coover, J. Dawson, W. Haberichter, E. Petereit (ANL/HEP)
Nucl. Inst. and Methods A274, 152 (1989).

A Stable, Rapidly Converging Conjugate Gradient Method for Energy Minimization
R. Hagstrom (ANL), S. Watowich et al. (Univ. of Chicago), E. Meyer (Harvard Univ.)
Jour. Computational Chemistry 9, 650 (1988).

Polarized Proton and Antiproton Beams at Fermilab and Associated Experiments
A. Yokosawa (ANL)
Mod. Phys. A3, No. 12, World Scientific Publishing Co., 2753 (1988).

Particle Production in Continuum e^+e^- Annihilation at High Energy
M. Derrick (ANL)
Book - Review Volume on Hadronic Multiparticle Production (1988).

Hadron Masses in Lattice Gauge Theories: The Inclusion of Dynamical Fermions
D. Richards (ANL)
Proceedings of the International Symposium on Field Theory on the Lattice, Seillac, France (1988).

Hybrid Simulations with Dynamical Quarks: Spectra, Screening and Thermodynamics
D. Sinclair (ANL)
Ibid. (1988).

Are There Bound Exotic Anticharmed Strange Baryons ($\bar{c}$suud and $\bar{c}$sudd)
H. Lipkin (ANL/Weizmann Inst.)
Proceedings of the International Symposium on the Production and Decay of Heavy Flavors, Stanford, CA (1988).

Advanced Accelerator Research at Argonne
R. Konecny, J. MacLachlan, J. Norem, A. Ruggiero, P. Schoessow, J. Simpson (ANL)
Proceedings of the International Conference on High Energy Accelerators, Novosibirsk, USSR, 132 (1988).

Characteristics of Multimuon Events from Fourth Generation Quarks at the SSC
H. Baer (ANL)
Proceedings of the Workshop on Experiments, Detectors and Experimental Areas for the Supercollider, Berkeley, CA, 172 (1988).

Angular Resolution in Underground Detectors and a Status Report of the Soudan 2 Nucleon Decay Detector
I. Ambats, D. Ayres, W. Barrett, K. Barron, J. Dawson, T. Fields, M. Goodman, F. Lopez, E. May, L. Price, J. Schlereth and J. Thron (ANL), H. Courant et al. (Univ. of Minnesota), W. Allison et al. (Oxford Univ.), J. Alner et al. (Rutherford-Appleton Laboratory), D. Benjamin et al. (Tufts Univ.)
Proceedings of the 2nd International Symposium on Underground Physics, Baksan, USSR, 242 (1988).

Are There Bound Exotic Anticharmed Strange Baryons ($\bar{c}$suud and $\bar{c}$sudd)
H. Lipkin (ANL/Weizmann Inst.)
Proceedings of the International Symposium on the Production and Decay of Heavy Flavors, Stanford, CA, edited by E.D. Bloom and A. Fridman, Annal of the New York Academy of Sciences 535, 438 (1988).

Heavy Quark Production in ep Collisions at HERA
M. Derrick (ANL)
Proceedings of the Workshop on High Sensitivity Beauty Physics at Fermilab, edited by A. Slaughter, M. Lockyer, M. Schmidt, 159 (1988).

Workshop on Detector Simulation for the SSC
L. Price, editor
Proceedings for the Workshop on Detector Simulation for the SSC, Argonne, IL (1988).

Some Implications of a Possible NNπ Bound State
H. Lipkin (ANL/Weizmann Inst.)
Proceedings of the 3rd Conference on the Intersections between Particle and Nuclear Physics, Rockport, Maine, edited by G.M. Bunce, AIP Conference Proceedings No. 176, 581 (1988).

Future Polarization Physics at Fermilab
E. L. Berger (ANL), J. G.MOrfin (FNAL), A. L. Read (FNAL), and A. Yokosawa (ANL), editors
Proceedings of the Symposium on Fugure Polarization Physics at Fermilab, FNAL (1988).

Future Plans for the MP Line (Both General and Specific)
D. G. Underwood (ANL)
Proceedings on Future Polarization Physics at Fermilab, Batavia, IL, 237 (1988).

A Long Polarized Target for the Fermilab Muon Beam
Harold Spinka (ANL)
Ibid., 243 (1988).

Flavor Symmetry and the Spin of the Proton
H. Lipkin (ANL/Weizmann Inst.)
Ibid., 261 (1988).

Orbital Angular Momentum and Parton Spin Densities
D. Sivers (ANL)
Ibid., 275 (1988).

$\Delta\pi_L$(pp) and Jet Physics
D. Richards (ANL)
Ibid., 309 (1988).

Nuclear Dependence of Structure Functions in the Shadowing Region of Deep Inelastic Scattering
E. Berger, J. Qiu (ANL)
Proceedings of the Topical Conference on Nuclear Chromodynamics, Argonne, IL, edited by J. Qiu and D. Sivers, published by World Scientific, 119 (1988).

Hyperfine Interactions, The Key to Multiquark Physics?
H. Lipkin (ANL/Weizmann Inst.)
Ibid., 260 (1988).

Nuclear Chromodynamics is not the Colorization of Nuclear Physics
D. Sivers (ANL)
Ibid., 283 (1988).

Reactions Probing Effects of Quark Clusters in Nuclei
K. Lassila (ANL/Univ. of Illinois), U. Kukhatme (Univ. of Chicago)
Proceedings of the Workshop on Nuclear and Particle Physics on the Light Cone, LAMPF, Los Alamos, NM, edited by M. Johnson, L. Kisslinger (1988).

B. Papers Submitted for Publication and ANL Reports

Study of b Quark Production and Decay in e^+e^- Annihilations at 29 GeV
S. Abachi, M. Derrick, P. Kooijman, J. Loos, B. Musgrave, L. Price, J. Repond, K. Sugano (ANL), C. Ng *et al*. (Purdue Univ.), D. Blockus (Indiana Univ.), C. Akerlof (Univ. of Michigan) ANL-HEP-PR-88-11
Phys. Rev. D

Searching for Supersymmetry at e^+e^- Supercolliders
D. Karatas (ANL/IIT), H. Baer (Florida State Univ.), A. Bartl *et al*. (Univ. of Wisconsin) ANL-HEP-PR-88-24
Int. Jour. Mod. Phys.

Inclusive Large Mass Muon Pair Production in Ultra-Relativistic Nucleus-Nucleus
L. Roberts (ANL) ANL-HEP-PR-88-33
Zeit. fur Phys.

Redundancy of Conditions for a Virasoro Algebra
J. Uretsky (ANL/College of DuPage) ANL-HEP-PR-88-41
Commun. Math Phys.

Experimental Measurements of Nonlinear Plasma Wakefields
J. Rosenzweig, P. Schoessow, B. Cole, W. Gai, R. Konecny, J. Norem, J. Simpson (ANL) ANL-HEP-PR-88-43
Phys. Rev. Lett.

Dynamical Chiral Symmetry Breaking in Strong Coupling Unquenced QED_4
J. Oliensis (ANL) ANL-HEP-PR-88-45
Phys. Rev. Lett.

Scenarios for Spin Physics and Parton Spin-Transfer Densities
D. Sivers, J. Qiu, D. Richards (ANL), G. Ramsey (ANL/Loyola)
ANL-HEP-PR-88-52
Phys. Rev. D.

Modulation of Continuous Electron Beams in Plasma Wakefields
James Rosenzweig (ANL) ANL-HEP-PR-88-53
Phys. Rev. Lett.

Trigonometric Structure Constants for New Infinite Algebras
C. Zachos (ANL), D. Fairlie, P. Fletcher (Univ. of Durham)
ANL-HEP-PR-88-56
Phys. Rev. B.

C. Zachos (ANL), D. Fairlie, P. Fletcher (Univ. of Durham)
ANL-HEP-PR-88-56
Phys. Rev. B.

Wake Field Acceleration Experiments
J. Simpson (ANL) ANL-HEP-CP-88-57
Proceedings of the Tenth Conference on the Application of Accelerators in Research and Industry, University of No. Texas, Denton, Texas, Nov. 7-9, 1988.

A New Derivation of the Altarelli-Parisi Equations
J. Qiu (ANL), J. Collins (Illinois Inst. of Technology)
ANL-HEP-PR-88-65
Phys. Rev. D.

"b-Spin", an SU(2) Symmetry for Describing B^0-B^0 Mixing, and CP Violation
H. Lipkin (ANL/Weizmann Inst.) ANL-HEP-PR-88-66
Nucl. Phys. B

Light Pipe Optical Joints Made from Silicone Disks
J. Loos (ANL), L. Rangan, E. Shibata (Purdue Univ.) ANL-HEP-PR-88-69
Nucl. Inst. and Methods

Some Continuously Variable Partial Snakes of Type I and Type II
D. Underwood (ANL) ANL-HEP-PR-88-71
Nucl. Inst. & Methods

The Perturbative QCD Corrections to the Ratio R for τ Decay
E. Braaten (ANL/Northwestern Univ.) ANL-HEP-PR-88-82
Phys. Rev. D. Brief Reports

Dynamic Polarization of ^{19}F in a Fluorinated Alcohol
D. Hill, T. Kasprzyk (ANL), J. Jarmer et al. (LANL), M. Krumpolc (Univ. of Illinois), G. Hoffmann et al. (Univ. of Texas)
ANL-HEP-PR-88-88
Nucl. Inst. and Methods

Measurement of the Branching Ratio for $\tau^- \rightarrow e^- \bar{\nu}_e \nu_\tau$
A. Abachi, M. Derrick, P. Kooijman B. Musgrave, L. Price, J. Repond, K. Sugano (ANL), D. Blockus et al. (Indiana Univ.), C. Akerlof et al. (Univ. of Michigan), P. Baringer et al. (Purdue Univ.) ANL-HEP-PR-88-89
Phys. Lett.

Production Cross Section and Topological Branching Fractions of the τ Lepton
A. Abachi, M. Derrick, P. Kooijman B. Musgrave, L. Price, J. Repond, K. Sugano (ANL/HEP), D. Blockus et al. (Indiana Univ.), C. Akerlof et al. (Univ. of Michigan), P. Baringer et al. (Purdue Univ.) ANL-HEP-PR-88-90
Phys. Rev.

Effects of Initial-State QCD Interactions in the Drell-Yan Process
G. Bodwin (ANL), S. Brodsky (SLAC) ANL-HEP-PR-88-91
Phys. Rev. D.

Observation of Structures in the Mass Range of 2700 to 2900 MeV in the Difference Between the pp Total Cross Sections for Pure Helicity States
I. Auer, E. Colton, W. Ditzler, H. Halpern, D. Hill, R. Miller, H. Spinka, N. Tamura, J. Tavernier, G. Theodosiou, K. Toshioka, D. Underwood, R. Wagner, A. Yokosawa (ANL) ANL-HEP-PR-88-96
Phys. Rev. Lett.

Multi-Fluid Models for Plasma Wake-field Phenomena
J. Rosenzweig (ANL/FNAL) ANL-HEP-PR-88-98
Phys. Rev. A.

Relief Device Sizing for the Helium Dewars Associated with the MP-9 Polarized Target
D. Hill, A. Buehring (ANL) ANL-HEP-TR-88-86
Technical Report

Relief Device Sizing for the Polarizing Solenoid of the MP-9 Polarized Target
D. Hill (ANL), P. Stone (FNAL) ANL-HEP-TR-88-87
Technical Report

A High Resolution Beam Profile Monitor Using Bremsstrahlung
J. Norem, P. Schoessow (ANL/HEP) ANL-HEP-TR-88-44
Technical Note

Notes of Pressure Relief Safety of Helium Containers
D. Hill (ANL) ANL-HEP-TR-88-95
Technical Report

C. Papers or Abstracts Contributed to Conferences

LN(S) Physics with CDF
R. Blair, S. Kuhlmann, W. Li, L. Nodulman, J. Proudfoot, F. Ukegawa, D. Underwood, R. Wagner, B. Wicklund (ANL), with CDF Collaboration
Proceedings of the 23rd Moriond Conference, Les Arcs, France (March 13-19, 1988).

A Measurement of Intermediate Vector Boson Production in 1.8 TeV $\bar{p}p$ llisions
R. Blair, S. Kuhlmann, W. Li, L. Nodulman, J. Proudfoot, F. Ukegawa, D. Underwood, R. Wagner, B. Wicklund (ANL), with CDF Collaboration
(Presented by R. St. Denis)
Proceedings of the 23rd Moriond Conference, Les Arcs, France (March 13-19, 1988).

Preliminary Results from CDF on W,Z Production at the Tevatron
R. Blair, S. Kuhlmann, W. Li, L. Nodulman, J. Proudfoot, F. Ukegawa, D. Underwood, R. Wagner, B. Wicklund (ANL), with CDF Collaboration
St. Croix Proceedings (1988).

Recent Results from the CDF Detector at Fermilab
R. Blair, S. Kuhlmann, W. Li, L. Nodulman, J. Proudfoot, F. Ukegawa, D. Underwood, R. Wagner, B. Wicklund (ANL), with CDF Collaboration
9th International Seminar on HEP Problems, Dubna, USSR (June 14-19, 1988).

Status Report on CDF
R. Blair, S. Kuhlmann, W. Li, L. Nodulman, J. Proudfoot, F. Ukegawa, D. Underwood, R. Wagner, B. Wicklund (ANL), with CDF Collaboration
Recontres de Physique de la Vallee D'Aoste on Results & Perspectives in Particle Physics, La Thuile, Aosta Valley, Italy (March 1-7, 1988).

First Events and Prospects at the Fermilab Collider
R. Blair, S. Kuhlmann, W. Li, L. Nodulman, J. Proudfoot, F. Ukegawa, D. Underwood, R. Wagner, B. Wicklund (ANL), with CDF Collaboration
Proceedings of Second Aspen Winter Particle Physics Conference (1986).

CDF Results and Prospects for Elastic Scattering
R. Blair, S. Kuhlmann, W. Li, L. Nodulman, J. Proudfoot, F. Ukegawa, D. Underwood, R. Wagner, B. Wicklund (ANL), with CDF Collaboration
7th Topical Workshop on $\bar{p}p$ Collider Physics, FNAL (June 20-24, 1988).

W Boson Production in pp Collisions at S = 1.8 TeV
R. Blair, S. Kuhlmann, W. Li, L. Nodulman, J. Proudfoot, F. Ukegawa, D. Underwood, R. Wagner, B. Wicklund (ANL), with CDF Collaboration
7th Topical Workshop on $\bar{p}p$ Collider Physics, FNAL (June 20-24, 1988).

Charged and Strange Inclusive Particle Production at the Fermilab Collider
R. Blair, S. Kuhlmann, W. Li, L. Nodulman, J. Proudfoot, F. Ukegawa, D. Underwood, R. Wagner, B. Wicklund (ANL), with CDF Collaboration
Arles Proceedings (1988).

Limits on the Masses of Supersymmetric Particles from 1.8 TeV $\bar{p}p$ Collisions
R. Blair, S. Kuhlmann, W. Li, L. Nodulman, J. Proudfoot, F. Ukegawa, D. Underwood, R. Wagner, B. Wicklund (ANL), with CDF Collaboration
XXIV International Conference on High Energy Physics, Munich, Germany (August 4-10, 1988).

Results on W-Z Physics from CDF
R. Blair, S. Kuhlmann, W. Li, L. Nodulman, J. Proudfoot, F. Ukegawa, D. Underwood, R. Wagner, B. Wicklund (ANL), with CDF Collaboration
XXIV International Conference on High Energy Physics, Munich, Germany (August 4-10, 1988).

Minimum Bias Physics at CDF
R. Blair, S. Kuhlmann, W. Li, L. Nodulman, J. Proudfoot, F. Ukegawa, D. Underwood, R. Wagner, B. Wicklund (ANL), with CDF Collaboration
Proceedings of Division of Particles and Fields Meeting, Storrs, CT (August 15-18, 1988).

Limits on the Masses of Supersymmetric Particles from 1.8 TeV PP Collisions
R. Blair, S. Kuhlmann, W. Li, L. Nodulman, J. Proudfoot, F. Ukegawa, D. Underwood, R. Wagner, B. Wicklund (ANL), with CDF Collaboration
Proceedings on VII Topical Workshop on Proton-Antiproton Collider, FNAL (June 20-24, 1988).

Inclusive Central Jets at the Tevatron $\bar{p}p$ Collider
R. Blair, S. Kuhlmann, W. Li, L. Nodulman, J. Proudfoot, F. Ukegawa, D. Underwood, R. Wagner, B. Wicklund (ANL), with CDF Collaboration
Proceedings on VII Topical Workshop on Proton-Antiproton Collider, FNAL (June 20-24, 1988).

Electroweak Physics at CDF
R. Blair, S. Kuhlmann, W. Li, L. Nodulman, J. Proudfoot, F. Ukegawa, D. Underwood, R. Wagner, B. Wicklund (ANL), with CDF Collaboration
Proceedings of Physics in Collision VIII Conference, Capri, Italy (Oct. 19-21, 1988).

A Presentation for Virasoro Algebras
C. Zachos (ANL) ANL-HEP-CP-88-49
Talk at the XVIIth International Colloquium on Group Theoretical Methods in Physics, Ste-Adele, Quebec, Canada (June 27-July 2, 1988).

A High Resolution Beam Profile Monitor Using Bremsstrahlung
J. Norem (ANL) ANL-HEP-CP-88-58
Proceedings of the 1988 Linac Conference, CEBAF, Williamsburg, VA (Oct. 2-7, 1988).

Calorimetry in ZEUS, Lessons for the Future
M. Derrick (ANL) ANL-HEP-CP-88-59
Proceedings of the 1988 Summer Study on High Energy Pnysics in the 1990's, Snowmass, CO (June 27-July 1, 1988).

Charm Production in e^+e^- Annihilation
M. Derrick (ANL) ANL-HEP-CP-88-60
Proceedings of the XXIV International Conference on High Energy Physics, Max-Planck Inst. fur Physik, Munich, W. Germany (August 4-10, 1988).

W Boson Production in pp Collisions at $\sqrt{s}$ = 1.8 TeV
J. Proudfoot for the CDF Collaboration ANL-HEP-CP-88-61
Proceedings of the 7th Topical Workshop on Proton-Antiproton Collider Physics, Fermi National Accelerator Laboratory (June 20-24, 1988).

Final Focus Plasma Lenses in Linear Collider
J. Rosenzweig (ANL), P. Chen (SLAC) ANL-HEP-CP-88-62
Proceedings of the Capri Workshop on Future Linear Colliders, Capri, Italy (June 13-17, 1988).

A Possible Early Experimental Test for a Large $\Delta G(x,Q^2)$
D. Sivers (ANL), G. Ramsey (ANL/Loyola Univ.) ANL-HEP-CP-88-63
8th International Symposium on High Energy Spin Shysics, Univ. of Minnesota, Minneapolis, MN (Sept. 7-16, 1988).

Heavy Flavor Production at Fixed Target and Collider Energies
E. Berger (ANL) ANL-HEP-CP-88-67
Proceedings of the 1988 Annual Meeting of the Division of Particles and Fields, Storrs, CT (August 15-18, 1988).

Phenomenology of Heavy Flavor Production
E. Berger (ANL) ANL-HEP-CP-88-68
Proceedings of the XXIV International Conference on High Energy Physics, Munich, Germany (August 3-11, 1988).

The Fermilab Polarized Beam Snake
D. Underwood (ANL) ANL-HEP-CP-88-70
Proceedings of the 8th International Symposium on High Energy Spin Physics, University of Minnesota, Minneapolis, MN (Sept. 12-17, 1988).

Dynamic Polarization of ^{19}F in a Fluorinated Alcohol
D. Hill, T. Kasprzyk (ANL), J. Jarmet et al. (LANL), M. Krumpolc (Univ. of Illinois at Chicago), G. Hoffman et al. (Univ. of Texas, Austin) ANL-HEP-CP-88-72
Proceedings of the 8th International Symposium on High Energy Spin Physics, University of Minnesota, Minneapolis, MN (Sept. 12-17, 1988).

Spin Models of the Proton
G. Ramsey (ANL) ANL-HEP-CP-88-73
Proceedings of the 8th International Symposium on High Energy Spin Physics, Minneapolis, MN (September 12-17, 1988).

Surprising Theoretical Results on the Decay Rate of the τ Lepton
E. Braaten (ANL/Northwestern) ANL-HEP-CP-88-74
Proceedings of the 1988 Annual Meeting of the Division of Particles and Fields, Storrs, CT (Aug. 15-18, 1988).

Progress Report on the Polarized Target for the Fermilab Spin Physics Facility
D. Hill (ANL), P. Chaumette et al (Cen-Saclay) ANL-HEP-CP-88-76
Proceedings of the 8th International Symposium on High Energy Spin Physics, University of Minnesota, Minneapolis, MN (Sept. 12-17, 1988).

Prototype VME Data Acquisition Card for the ZEUS Calorimeter
J. Dawson, J. Berg, J. Schlereth, R. Stanek (ANL) ANL-HEP-CP-88-77
Proceedings of the IEEE 1988 Nuclear Science Symposium, Orlando, FL (Nov. 9-11, 1988).

Polarized Proton and Antiproton Experiments at Fermilab E-581/704
A. Yokosawa (ANL) ANL-HEP-CP-88-78
Proceedings of the 8th International Symposium on High Energy Spin Physics, University of Minnesota, Minneapolis, MN (Sept. 12-17, 1988).

Theory of Intrabeam Scattering in Strong-Focussing Accelerators
S.K. Mtingwa (ANL) ANL-HEP-CP-88-79
Proceedings of the First Edward Bouchet International Conference on Physics and Technology, International Center for Theoretical Physics, Trieste, Italy (1988).

The Finite Temperature Behavior of Lattice QCD with Moderate to Large Quark Masses
D. Sinclair (ANL) ANL-HEP-CP-88-80
Nuclear Physics B Proceedings Supplements Section, Proceedings of the 1988 Symposium on Lattice Field Theory, Fermilab, Batavia, IL (Sept. 22-25, 1988).

The QCD Vacuum at Infinite Momentum
A. White (ANL) ANL-HEP-CP-88-81
Proceedings of the "Hadronic Matter in Collision" Conference, Univ. of Arizona, Tucson, AZ (Oct. 6-12, 1988).

Analysis of a Lattice Wess-Zumino Scheme for Chiral Fermions
G. Bodwin, E. Kovacs (ANL) ANL-HEP-CP-88-83
Proceedings of the 1988 Symposium on Lattice Field Theory, Fermilab, Batavia, IL (Sept. 22-25, 1988).

Fermionic Center in the Superconformal Algebra on the Supertorus
C. Zachos (ANL) ANL-HEP-CP-88-84
Proceedings of the IV International Workshop on Recent Developments in High Energy Physics, Orthodox Academy of Crete, Crete, Greece (July 2-10, 1988).

Quarks and the Spin of the Proton for Pedestrians
H. Lipkin (ANL/PHY/Weizmann Inst.) ANL-HEP-CP-88-92
Proceedings of the Excited Baryons- 1988 Conference, Rensselaer Polytechnic Inst., Troy, NY (August 4-6, 1988).

Towards an Understanding of the Nuclear Potential
D. Sivers, D. Sinclair (ANL), D. Richards (Univ. of Edinburgh)
ANL-HEP-CP-88-93
Proceedings of the International Symposium Lattice '88, Fermilab, Batavia, IL (Sept. 22-25, 1988).

D. Technical Notes

AMZEUS-66 EGS Calculations for the ZEUS Barrel Shower Counters II
J. Repond

AMZEUS-67 Orpheus Harp II
E. Balabanis, M. Derrick, N. Hill, L. Kocenko, J. Repond

AMZEUS-68 ZEUS BCAL Field Mapping
R. Rezmer, R. Stanek

AMZEUS-69 Test Results of the Drift Tubes for the Cosmic Ray Calibration at ANL
I. Ambats, P. MacLean, B. Musgrave, K. Sugano

AMZEUS-70 Dimensional Specification of HAC Scintillator Tiles
S. Durkin, B. Musgrave, E. Petereit

AMZEUS-71 Notes on a Meeting of the U.S. ZEUS Collaboration
M. Derrick

AMZEUS-72 Specifications for the Depleted Uranium Plate Contract
B. Musgrave

AMZEUS-73 Dimensional Checking of Prototype DU Plates
R. Rezmer, S. Kaminskas, D. Litzenberg, B. Musgrave

AMZEUS-74 VME/CAMAC Interface
J. Dawson, J. Berg, J. Schlereth, R. Stanek

AMZEUS-75 Use of the TMS32010 Digital Signal Processor in the Calibration System
J. Schlereth

AMZEUS-76 Trigger Logic and Electronics for the Cosmic Ray Test Stand
K. Sugano

CDF-709 Steps in Deriving the Inclusive Jet Cross Section
S. Kuhlmann

CDF-710 Run-List for the Inclusive Jet Cross Section
S. Kuhlmann

CDF-711 Acceptance Issues for the Inclusive Jet Cross Sections
S. Kuhlmann

CDF-725 Single Phototube Trigger Rates in the Central E-M Calorimeter
R. Wagner

CDF-759 The Level 3 Missing ET Trigger and its Generalizations
L. Nodulman

CDF-760 Proposal for a Preradiator Chamber for the CDF Central Detector
R. Blair, S. Kuhlmann, L. Nodulman

CDF-775 Summary of Results on Radiative W Decay
R. Wagner

CDF-776 Dijet Angular Distributions from PBARP Collisions at Root S = 1.8 TeV
R. St. Denis

CDF-783 Recent Results from the CDF Detector at Fermilab
R. Blair, S. Kuhlmann, W. Li, L. Nodulman, J. Proudfoot, F. Ukegawa, D. Underwood, R. Wagner, B. Wicklund

CDF-790 A Level 3 Photon Filter
R. Blair, A. Bamberger

CDF-828 Recent Results: Collider Detector at Fermilab
R. Blair, S. Kuhlmann, W. Li, L. Nodulman, J. Proudfoot, F. Ukegawa, D. Underwood, R. Wagner, B. Wicklund

CDF-832 Missing ET Data Sets 1988
W. Trischuk, L. Nodulman

CDF-837 Compositeness Limits from 1987 Dijet Angular Distribution Data
R. St. Denis

CDF-839 Missing ET Dijet Cut
L. Nodulman

CDF-840 Crack Chambers Live
L. Nodulman

CDF-846 Scan of a Subset of 1 Inverse Picobarn of Zen Missing ET Data
L. Nodulman

CDF-860 Preinstallation Validation of Level 3 Filter Cepflt
J. Proudfoot

CDF-862	Preliminary Look at 1988 Jet Data: Dijet KT and DN/DCOS R. St. Denis
CDF-863	Implementation of Rate Checking in YMON for the 88 Run L. Nodulman
PDK-371	A Method for Measuring the Leakage Current Parameter λ M. Saulnier, M. Goodman
PDK-372	Module 46 Test Stand Results and Field Measurements M. Saulnier
PDK-373	Soudan 2 Nucleon Decay Experiment Quarterly Activity Report - April-June 1988 D. Ayres
PDK-374	The Soudan Connections J. Thron
PDK-376	Summary of Decisions Taken at the Soudan 2 Collaboration Meeting, Tower, MN, July 25-27, 1988 D. Ayres
PDK-377	INTRANUKE: A Phenomenological Code for Pion Rescattering Within An Extended Nucleus W.A. Mann, T. Vu, R. Merenyi, W. Barrett
PDK-382	Soudan 2 Nucleon Decay Experiment Quarterly Activity Report, July-September 1988 D. Ayres
PDK-383	Measurement of Air Circulation, Radon, and Carbon Dioxide at the Soudan Minnesota Physics Laboratory D. Jankowski
PDK-385	Nucleon Decay and Other Physics Reference List M. Goodman
PDK-386	Measurements of the Resistivities of Module Materials and a Surface Current Model B. Anderson
WF-86	Deposition of Beam Energy in a Metallic Box S. Mtingwa
WF-87	Summary of the Dielectric Wake Field Experiments W. Gai, P. Schoessow, B. Cole

WF-88	A High Resolution Beam Profile Monitor Using Bremsstrahlung J. Norem, P. Schoessow	
WF-89	Experimental Demonstration of Wake-field Effects in Dielectric Structures W. Gai, P. Schoessow, B. Cole, R. Konecny, J. Norem, J. Rosenzweig, J. Simpson	
WF-90	Longitudinal Space Charge Effects Near a Laser Photocathode J. Rosenzweig	
WF-91	Experimental Measurement of Nonlinear Plasma Wake-Fields J. Rosenzweig, P. Schoessow, B. Cole, W. Gai, R. Konecny, J. Norem, J. Simpson	
WF-92	Modulation of Continuous Electron Beams in Plasma Wake-fields J. Rosenzweig	
WF-93	Plasma Wake-Field Amplitudes from Self-Pinched Beams J. Rosenzweig	
WF-94	Final Focus Plasma Lenses in Linear Colliders J. Rosenzweig	
WF-95	High Resolution Beam Profile Monitors for the Final Focus of Linear Colliders J. Norem	
WF-96	Plasma Lens Valve Nozzle Tests J. Norem, R. Konecny	
WF-97	Instability of Compensated Beam-Beam Collision J. Rosenzweig	
WF-98	Multi-Fluid Models for Plasma Wake-Field Phenomena J. Rosenzweig	

VII. HIGH ENERGY PHYSICS RESEARCH PERSONNEL

Accelerator Physicists

S. Mtingwa
J. Norem
J. Rosenzweig
P. Schoessow
J. Simpson

Experimental Physicists

D. Ayres
R. Blair
M. Derrick
T. Fields
A. Gabutti
R. Garnett
M. Goodman
W. Gai
D. Grosnick
R. Hagstrom
F. Lopez
D. Lopiano
E. May
B. Musgrave
L. Nodulman
Y. Ohashi
L. Price
J. Proudfoot
J. Repond
T. Shima
H. Spinka
R. Stanek
K. Sugano
J. Thron
D. Underwood
R. Wagner
A. B. Wicklund
A. Yokosawa

Theoretical Physicists

P. Arnold
E. Berger
G. Bodwin
J. W. Qiu
D. Sinclair
D. Sivers
A. White
C. P. Yuan
C. Zachos

Engineers, Computer Scientists and Applied Scientists

A. Buehring
J. Dawson
D. Hill
N. Hill
J. Schlereth
W. Wang

Technical Support Staff

I. Ambats
L. Balka
J. Biggs
H. Blair
W. Haberichter
D. Jankowski
T. Kasprzyk
R. Konecny
R. Laird
R. Miller
R. Rezmer
J. Sheppard

Laboratory Graduate Participants

C. Ho
D. Karatas
D. Keubel
M. Laghai
C. Nantista
F. Ukegawa

Appendix A
COLLOQUIA AND CONFERENCE TALKS

P. Arnold

"Baryon Number Nonconservation in Electroweak Theory"
Univ. of Minnesota (October 1988)
C.I.E.A., Mexico City (November 1988)
Univ. of Pennsylvania (December 1988).

E. Berger

"Heavy Quark Production at Fixed-Target and Collider Energies".
University of Chicago, Enrico Fermi Institute (November 1988)

"Heavy Quark Production at Fixed Target and Collider Energies."
Indiana University, High Energy Physics Seminar (October 1988).

"Heavy Quark Production at Fixed Target and Collider Energies".
Centre d'Etudes Nucleaires de Saclay, Département de Physique des Particules Elémentaires, Saclay, France. Séminaire du Département. (September 1988).

"Heavy Quark Production at Fixed Target and Collider Energies".
Laboratoire de Physique Théorique et Particules Elémentaires, Université de Paris-Sud, Orsay, France (September 1988).

"High Twist Contributions in Massive Lepton Pair Production and in Hadronic Jet Production" (Invited Review)
Workshop on Higher Twists and High p_T Physics, College de France, Paris (September 1988).

"High Twist Contributions in Semi-inclusive Deep Inelastic Lepton Scattering" (Invited Review)
Workshop on Higher Twists and High p_T Physics, College de France, Paris (September 1988).

"Review of the XXIV International Conference on High Energy Physics, Munich"
High Energy Physics Division, Argonne National Laboratory (August 1988).

"Phenomenology of Heavy Quark Production" (Invited Review)
Annual Meeting of the Division of Particles and Fields, American Physical Society, University of Connecticut, Storrs, CT (August 1988).

"Phenomenological Aspects of Heavy Quark Production" (Invited Review)
XXIV International Conference on High Energy Physics, Munich (August 1988).

"Shadowing and the EMC Effect" (Invited Review)
XXIV International Conference on High Energy Physics, Munich (August 1988).

"Diffractive Production of Heavy Quarks, W's, and Jets".
Summer Study on High Energy Physics in the 1990's, Snowmass, Colorado (July 1988).

M. Derrick

"Calorimetry in ZEUS:Mesons for the Future"
Summer Study on High Energy Physics in the 1990's, Snowmass, Colorado (July 1988).

"Charm Production in Continuum e^+e^- Annihilation"
XXIV International HEP Conference, Munich (August 1989).

T. Fields

"Jet Production in pA Collisions at 400 GeV"
Univ. of Science and Technology, Heifei, China (October 1988).

A. Gabutti

"Superconducting Detectors, First Experimental Results"
National Institute of Standards and Technology, (October 1988).

P. Job

"EGS Applications to Thin Layer Geometry"
KFA Julich, W. Germany (October 1988).

D. Karatas

"Supersymmetry at the SSC"
JINR, Dubna (September 1988).

L. Nodulman

"Hadron Collider Physics"
Beyond the Standard Model Workshop, Ames, Iowa (November 1988).

L. Price

"Summary of the HEPNET Review Committee Report"
HEPAP Meeting, Snowmass, CO (July 1988)

"Status Report on Detector Simulation Tools for SSC Experiments"
Workshop on Future Directions in Detector R&D for Experiments at pp Colliders, Snowmass, CO (July 1988)

D. Underwood

"The Fermilab Polarized Beam Snake"
Siberian Snake Workshop, Minneapolis, MN (September 1988).

J. Norem

"The Development of Plasma Lenses"
Topical Conference on Submicron Beams, Santa Barabara, CA (July 1988).

J. Qiu

"Twist-4 Contributions to Parton Distributions"
"Shadowing Effect in Nuclear Parton Distributions"
Iowa State Univ. Ames, Iowa (October 1989).

"Understanding Nucleon Shadowing at Parton Level"
Univ. of Tennessee, Oak Ridge National Laboratory (July 1988).

H. Spinka

"The LAMPF Nucleon-Nucleon Program"
Univ. of Manitoba (October 1988).

"The FNAL Polarized Beam Project"
Serpukhov, USSR (September 1988).

R. Wagner

"Development of a Superconducting Vertex Detector"
Argonne HEP Division Colloquium (December 1988).

A. White

"The QCD Vacuum at Infinite Momentum"
Conference on Hadronic Matter in Collision, Tucson, AZ (October 1988).

"Multi Regge Theory and the Infra-Red Analysis of QCD"
Warsaw-Stefan Banach Institute (November 1988).

A. Yokosawa

"Polarized Beam Experiments at Fermilab"
Minneapolis, MN (September 1988).

"Fermilab E-581/704 Experiments"
McGill Univ., Montreal, Canada (October 1988).

C. Zachos

"Fermionic Center in the Superconformal Algebra on the Supertorus"
IVth International Workshop in High Energy Physics, Crete, Greece (July 1988).

Appendix B
HIGH ENERGY PHYSICS COMMUNITY ACTIVITIES

E. Berger

International Advisory Committee and Organization Committee, "High Transverse Momentum Physics and Higher Twist Processes", College de France, Paris, September 1988.

Scientific Program Committee, XXIV Recontre de Moriond, "New Results in Hadronic Interactions", LesArcs, France, March 1989.

Elected Vice-chairman, Executive Committee, Division of Particles and Fields, American Physical Society, 1988.

Program Chairman, Division of Particles and Fields, American Physical Society, 1989. Responsible for the organization of invited paper sessions in Particles and Fields at the Spring Meeting of the APS, Baltimore.

L. Nodulman

R. St. Denis Ph.D. Thesis Committee.

L. Price

ESNET Steering Committee.

SSC Computing Task Force.

International Advisory Committee for Generic Detector R&D for the SSC.

Organizing Committee, IEEE Nuclear Science Symposium.

H. Spinka

Session Organizer for Minneapolis Spin Conference (September 1988).

External Ph.D. Thesis Examiner for Univ. of Manitoba student.

Member of Ph.D. Thesis committees for two New Mexico State U. students.